Science Engineering **Technology at AWE**

Discovery 23

July 2012

This issue:

Diamond Anvil Cell

High Current Pulsed Power Material Testing using AMPERE

Nuclear Data for Neutronic Systems Modelling

Research into Information Barrier Systems

Discovery

Contents

Cover image:
Diamond Anvil Cell

23

It is my pleasure in welcoming you to the 23rd issue of Discovery.

I am extremely proud to lead a team at AWE in which we have scientists and engineers who have received international acclaim for their research, innovation and discoveries. My career at AWE spans over 25 years, and I continue to be impressed by the dedication, professionalism and commitment of our diverse scientific, engineering and technical communities who work together to support the United Kingdom's nuclear deterrent.

Today, we are indeed recognised for our leadership in many areas of science, engineering and technology and we continue to strive for excellence as we meet the technical challenges of the future set against an ever changing external environment. It is essential that we are able to deliver science, engineering and technological solutions to support the Ministry of Defence and the UK Government as a trusted partner.

Orion, our new replacement laser facility; Blackthorn, one of the most powerful supercomputers in the UK; our state-of-the-art virtual reality suite; and AWE's collaboration with French colleagues in the field of hydrodynamics under the Anglo-French Treaty are just some of the areas through which we continue to demonstrate our commitment to innovation and science. This builds on the excellent and growing relationships we have with our US colleagues and the acclaim we receive for our work in science and technology.

Discovery was launched in 2000 and our vision for this publication remains unchanged: to be recognised for world standards of excellence in innovative science and technology.

The articles in this issue illustrate the richness and complexities of our technical programme to support nuclear deterrence and national security, working with stakeholders across UK Government, industry and academia.

I hope you enjoy reading Discovery and obtain an insight of the work carried out at AWE and the experts representing their fields.

Doctor Andrew Jupp
AWE Managing Director

Diamond Anvil Cell

The diamond anvil cell (DAC) is a pressure generating device used by researchers in academia and industry to compress materials to extremes of pressure. The DAC can be used to provide AWE with high pressure data for the validation of material modelling codes.

Pressure possesses perhaps the greatest range of all the physical variables; approximately 60 orders of magnitude separate the pressure in the remotest vacuum of space from that found at the centre of a neutron star [1].

High pressure conditions are frequently described as 'extreme' or 'abnormal', yet the pressure conditions we depend on for life are found in only a thin layer at the surface of the Earth and other planets. The pressure of the air in which we live is defined as one atmosphere. The centre of the Earth is at a pressure of approximately 3.5 million atmospheres (or 350 GPa), and more than 90% of the matter in the solar system exists at pressures above one million atmospheres (approximately 100 GPa).

Pressure thus shapes the interiors of stars and planets, including the Earth. It can convert everyday liquids such as water into spectacular crystals, and turn common gases into exotic metals and coal into diamonds. It is this ability to create remarkable new materials, particularly diamond, that has been the principal driving force behind high pressure science for the last two centuries [2].

In that time, the maximum static pressure obtainable in the laboratory has risen from a thousand atmospheres to several million atmospheres, while dynamic pressures as high as 10^{14} atmospheres have been created in thermonuclear explosions.

At AWE, extreme pressures are applied to study the structural response of materials (principally simple metals and alloys) in both the dynamic and static regimes.

Gas guns, explosives and high powered lasers are all employed in the generation of dynamic, or shock compression, data that can be used to validate equation of state (EOS) models [3,4].

Static high pressure data can be generated using diamond anvil cells, which access regions of phase space (pressure as a function of volume and temperature) that cannot be reached using the traditional dynamic methods. Thus the DAC plays an important role in the materials modelling community through the provision of static high pressure EOS data that complements data generated using dynamic methods.

How does it work?

Diamond is perfectly suited to high pressure experimentation. Firstly, it is the hardest known material. Secondly, diamond is transparent across much of the electromagnetic spectrum (ultraviolet, visible, infrared and X-ray). As a result, diamonds can be employed as anvils in high pressure devices unparalleled in their versatility. Using diamond anvils, materials can be volume compressed to millions of atmospheres whilst simultaneously having their properties interrogated using a broad range of experimental techniques.

The concept of fluid pressure (P) can be described as:

$$P = \frac{F}{A}$$

where A is the area (m^2) of a finite plane surface and F is the force in Newtons acting normal to that surface. For a simple piston and cylinder device, such as that shown in Figure 1, an applied force will squeeze the sample located between the piston and cylinder according to this

FIGURE 1

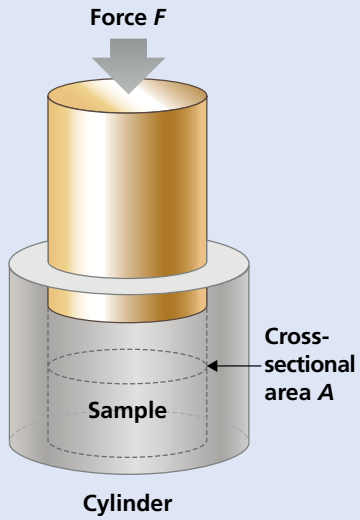

Generating pressure using a frictionless piston and cylinder device.

FIGURE 2

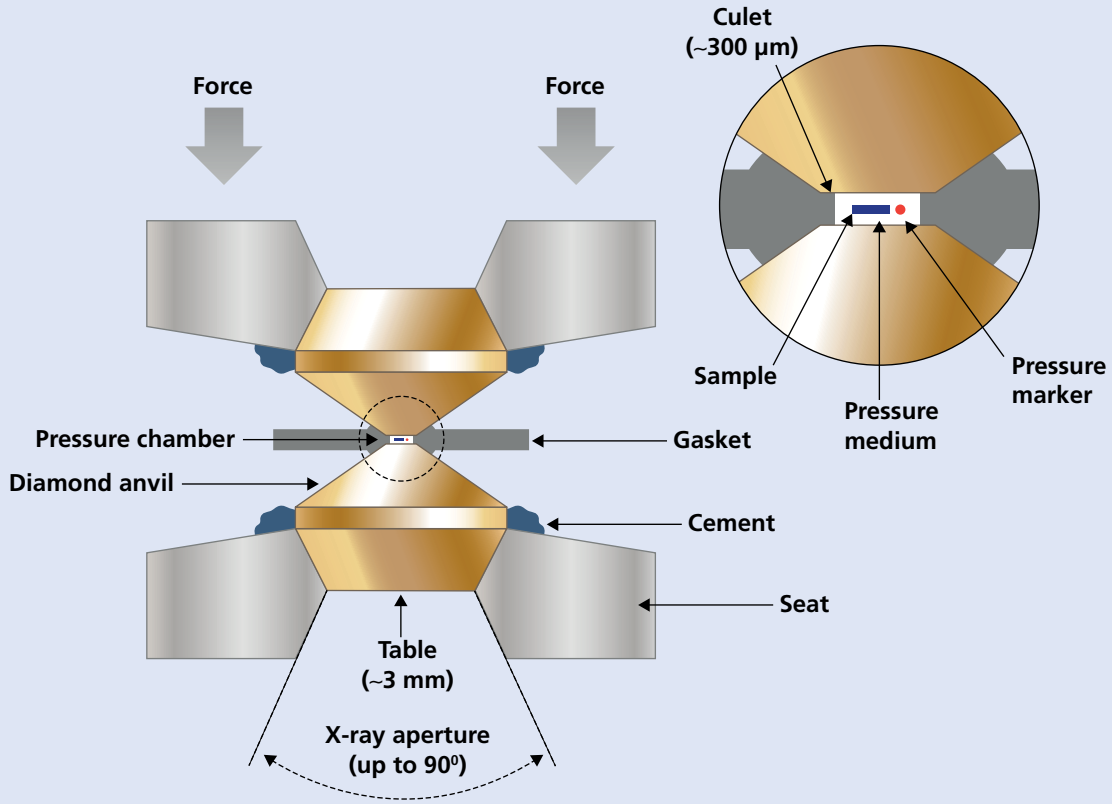

A schematic of the cross-sectional view of a DAC. The enlargement shows the placement of the sample and pressure marker in the pressure medium.

expression. The sample volume decreases as the pressure is increased.

If the piston has a small diamond fixed to its underside, the surface area through which the external force acts has suddenly reduced significantly. As a consequence, only a moderate force is required to generate a considerable pressure. This principle describes how pressure is generated in a DAC. Figure 2 shows a schematic of the cross-sectional view of a DAC.

Two opposed gem quality diamond anvils (each a third of a carat) are cemented into tungsten carbide seats, and aligned so that the culets (the flat face on the diamond parallel to the table) of the diamonds are perfectly parallel and concentric. Culet diameters typically vary between 50 µm and 400 µm depending on the pressure required in the experiment. An opening through the middle of both seats allows optical and X-ray access to both diamonds, and therefore to the sample. A thin (5-30 µm) metal gasket (typically constructed out of rhenium), with a small hole drilled through its centre (the diameter of which is approximately one third of the diameter of the culet) is held

"Only a moderate force is required to generate a considerable pressure."

between the two diamonds. As the diamonds are pushed together by an external force, the gasket deforms plastically around both culets to create a pressure chamber. The pressure chamber contains the sample under study, and this is usually embedded in a pressure transmitting medium (PTM). The function of the PTM is to ensure the sample experiences an almost hydrostatic pressure during compression – though sometimes, it is expedient not to use a PTM.

The choice of PTM is highly dependent on the type of experiment being considered. For example, a room temperature volume compression experiment would typically use a PTM that is quasi-hydrostatic, experiences no phase changes over the pressure range of interest, and is also non-reactive with the sample. Solid helium, neon and argon are commonly used in such room temperature compression experiments.

Experiments that involve heating of the sample, for example laser-heating, require some form of thermal insulation between the sample and the diamonds to prevent heat being conducted away from the sample. Aluminium oxide (Al_2O_3) and sodium chloride (NaCl) are good thermal insulators and are therefore used routinely in high temperature experiments.

A pressure marker is also included inside the pressure chamber, alongside the sample. Pressure can be determined either optically, by measuring the wavelength of the fluorescence emitted by the marker (for example, if the marker is a ruby crystal) when illuminated with a laser, or by using X-ray diffraction (if the marker has a well known EOS, for example, copper or tantalum).

Sample sizes in DAC experiments are necessarily very small. The limiting factor is the diameter of the diamond culets. For a culet diameter of 100 μm, it is possible to achieve a pressure of approximately 100 GPa, but the sample diameter will probably not exceed 20-30 μm and will be only 5 μm thick. By comparison, the diameter of a typical human hair is approximately 100 μm. The highest reported pressure attained using a DAC is 416 GPa, for which diamonds with culet diameters of

FIGURE 3

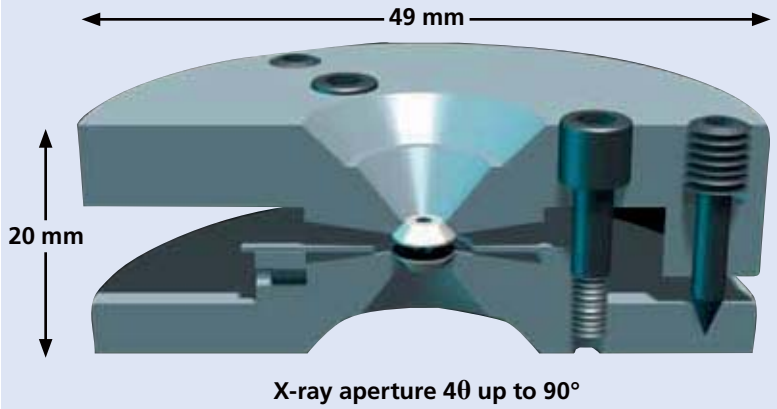

A cross-sectional view through an Almax Plate DAC.

FIGURE 4

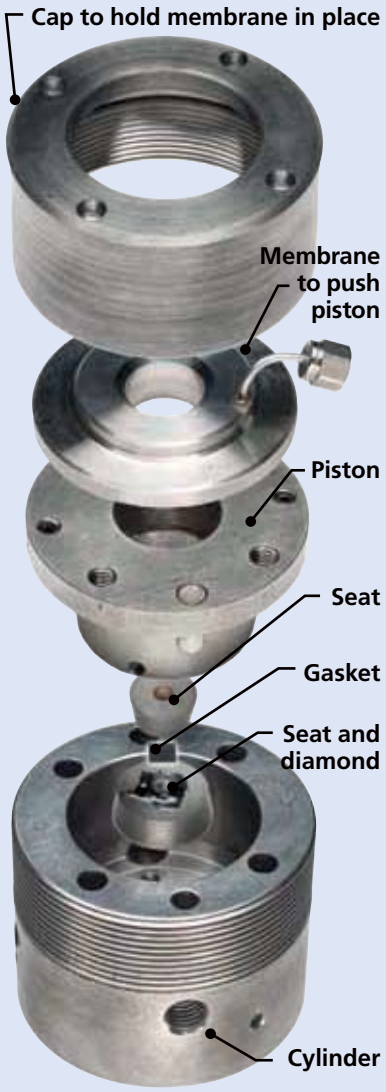

An exploded view of a DAC. A LLNL designed gas membrane cell.

21 µm and 23 µm were used [5]. The pressure limit inherent in diamond anvils has been calculated to fall between 350 GPa and 420 GPa [6]. DACs used by AWE are shown in Figures 3 and 4. In Figure 3, the Almax Plate DAC is a manually driven DAC with a large X-ray aperture. The exploded DAC shown in Figure 4 is a gas membrane driven device designed by the Lawrence Livermore National Laboratory (LLNL) High Pressure Group.

The hardness and transparency of diamond have resulted in DACs being incorporated into a variety of experiments, across a wide range of scientific disciplines, for which pressure is a useful variable. Solids, liquids and gases can all be compressed to megabar (100s of GPa) pressures. X-ray diffraction, X-ray absorption, Raman scattering, Brillouin scattering, Mössbauer spectroscopy, resistivity, magnetic susceptibility, cryogenic cooling, resistive heating and laser heating are among the many techniques that have been successfully adapted for high pressure DAC experiments [7].

FIGURE 5

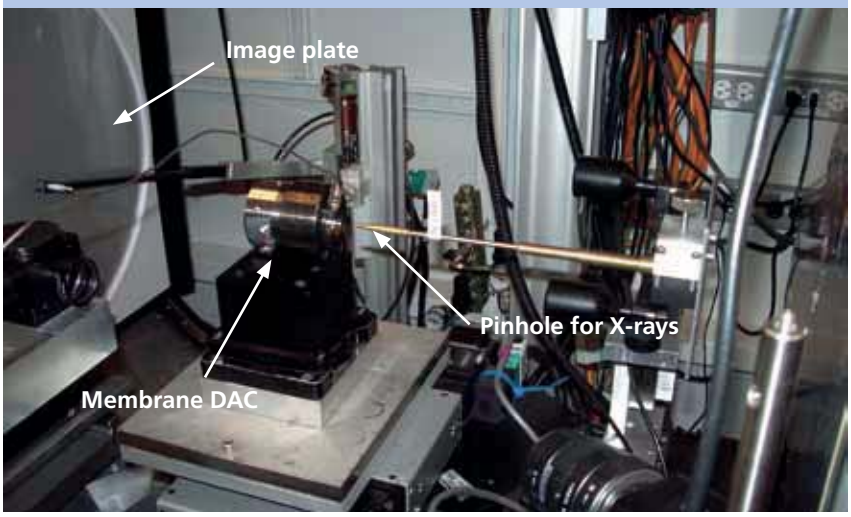

A membrane DAC at the high pressure beamline 16-ID-B.

Generating equation of state data

The EOS of a solid can be defined in terms of the three thermodynamic parameters: pressure (P), volume (V) and temperature (T), through the expression:

$$V = V(P, T)$$

The volume and volume change of a sample can be measured accurately using X-ray diffraction. Although X-ray diffraction patterns can be collected using commercially available diffractometers, these systems produce X-rays of such low intensity for DAC applications that there is a limit to what can realistically be achieved.

Exposure times for some refractory metals can be as long as many hours, or even days. This time constraint effectively prohibits the collection of high temperature pressure data and prevents the observation of any kinetic changes that may be taking place in the material. DAC experiments require very high intensity X-rays, short exposure times and micro-focussing. These capabilities are only available at a third generation synchrotron facility, such as the Advanced Photon Source in Chicago as described in Box 3.

Today, most static high pressure EOS experiments are performed

"The hardness and transparency of diamond have resulted in DACs being incorporated into a variety of experiments, across a wide range of scientific disciplines, for which pressure is a useful variable."

"DACs are more than just a piston and cylinder device for the generation of high pressures. The DAC is a versatile tool that is routinely used by researchers to study materials properties to millions of atmospheres across many disciplines."

at dedicated high pressure beamlines at these third generation synchrotrons, and the data are collected in the angle dispersive X-ray diffraction (ADXRD) mode. Figure 5 shows a membrane DAC installed at the high pressure beamline 16-ID-B at the Advanced Photon Source.

The ultimate pressure attained in an experiment is dependent on the type of experiment being performed and on the configuration of the DAC. For the EOS of metals, it is usual to compress the sample to as high a pressure as possible, at which point one or both diamonds in the DAC breaks.

The ADXRD patterns generated and collected at the beamline are then processed for analysis, as discussed in Box 1.

Magnesium test case

Alkali and alkaline earth metals are interesting systems for researchers because of their simple electronic structure. This makes them attractive as computational and theoretical test cases in understanding the behaviour of metals at extremes of pressure.

Sodium, potassium and calcium have been shown to possess complex crystal structures at pressures greater than 100 GPa [8-10], but no complex structures have been predicted for magnesium at similar pressures. However, magnesium is different from these systems as it is the only group I or II element to crystallise in the hexagonal-close packed (hcp) structure at ambient conditions. But does it also possess unexpected complex structures above 100 GPa?

In order to know the EOS, it is vital to correctly determine the crystal structure. Figure 6 shows the possible transformation pathway for magnesium under various pressures. At room temperature, magnesium transforms from hcp to the body-centred cubic (bcc) crystal structure at approximately 50 GPa [11-13]. The bcc structure is predicted

FIGURE 6

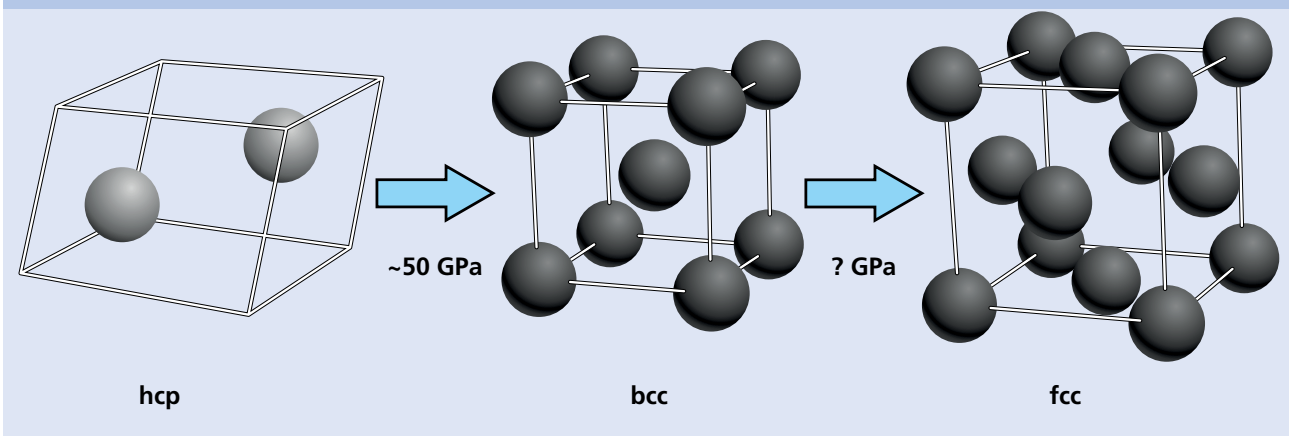

Possible room temperature transformation pathway for magnesium.

BOX 1

Crystal lattices

The elastic scattering of X-rays from a crystal structure is represented in Figure 7. The scattering of X-rays is described by Bragg's law:

$$\lambda = 2d_{hkl} \sin\theta$$

where λ is the wavelength of the radiation, d is the spacing of the atomic planes (using the Miller indices h, k, l), and 2θ is the angle between the incoming X-ray beam and the diffracted beam.

FIGURE 7

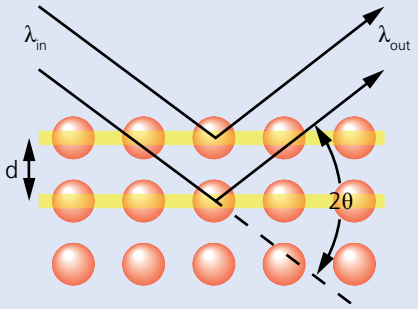

Scattering of X-rays from a crystal structure. The successive planes of atoms behave like a diffraction grating, resulting in an interference pattern.

Imaginary atomic planes are highlighted in yellow in Figure 7. Where these planes intersect the x, y and z axes defines their unit length in terms of the unit cell axes a_1, a_2 and a_3. The unit cell is the simplest arrangement of atoms that are periodically repeated throughout a crystal lattice. The intercepts of any (h, k, l) plane with the unit cell axes are labelled according to the following convention

$$h = \frac{a_1}{h'}, = \frac{a_2}{k'}, = \frac{a_3}{l'}$$

where h' is the intercept of the plane along the unit cell axis a_1 (the x-axis), k' is the intercept of the plane along the unit cell axis a_2 (the y-axis), and l' is the intercept of the plane along the unit cell axis a_3 (the z-axis). For the simplest case of a cubic lattice, the two examples in Figure 8 show the (110) and (210) lattice planes for the unit cell.

FIGURE 8

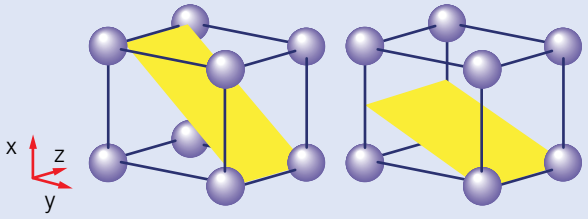

Lattice planes for a unit cell.

The diffraction of X-rays from lattice planes produces a pattern of intensities through constructive interference. For a polycrystalline material, Debye-Scherrer rings of intensity are formed on an image plate or charge coupled device (CCD), as shown in Figure 9.

The positions and intensities of the rings contain information on dimensions of the unit cell, and on the arrangement of the atoms within that cell, respectively. Each ring on the image plate corresponds to a particular lattice spacing d, or lattice plane (h, k, l).

FIGURE 9

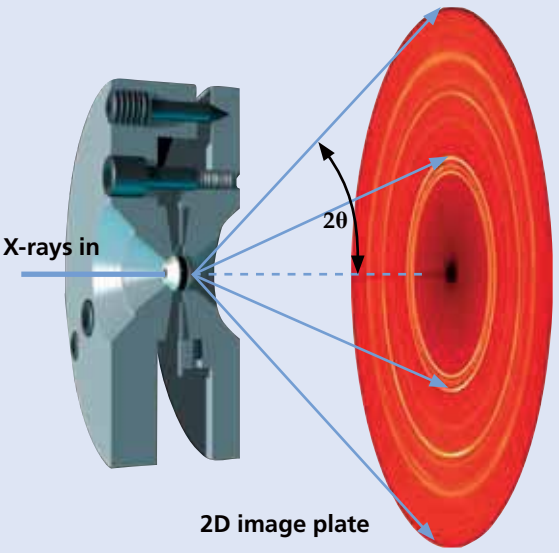

Illustration of the diffraction of X-rays from a DAC (an Almax Plate DAC in cross-section) onto an image plate.

BOX 1 continued

The 2D diffraction pattern collected by the image plate can then be simplified for data analysis by integrating azimuthally around the diffraction rings to produce a 1D intensity profile as shown in Figure 10.

FIGURE 10

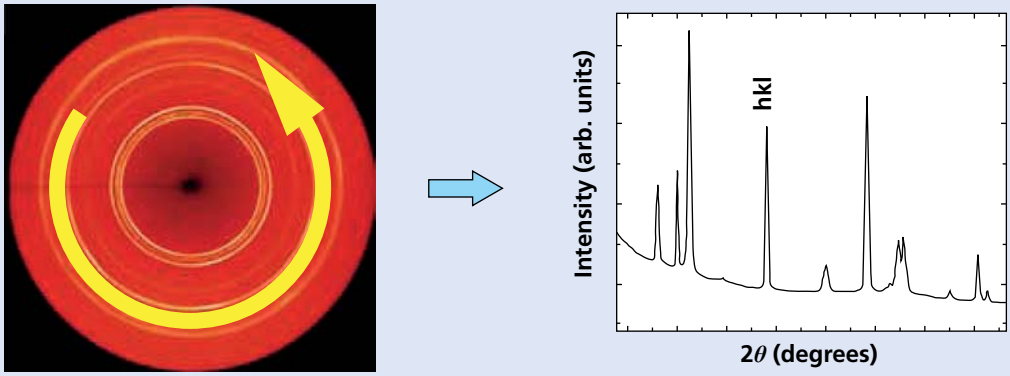

The process to convert a X-ray diffraction pattern from a 2D to a 1D format.

The 1D intensity profile is output as a plot of intensity against either scattering angle (degrees) or interplanar separation. There are many software packages available that can be used to identify and analyse the crystal structures of materials from their integrated diffraction patterns.

BOX 2

The equation of state

Although there is no absolute thermodynamic basis for choosing an empirical EOS for high pressure data analysis, the two most commonly used EOS formulae are the Birch-Murnaghan and the Vinet. For room temperature compression data, the 3rd order isothermal Birch-Murnaghan EOS is given by:

$$P_{BM}(V) = \frac{3}{2}B_0\left(\eta^{-7/3} - \eta^{-5/3}\right)\left[1 + \frac{3}{4}\left(B' - 4\right)\left(\eta^{-2/3} - 1\right)\right]$$

where $P_{BM}(V)$ is the pressure as a function of volume (or density), B_0 is the zero pressure bulk modulus, B' is the pressure derivative of the bulk modulus, and $\eta = V/V_0$ is the compression ratio, where V_0 is the zero pressure volume. The bulk modulus is a measure of the incompressibility (or hardness) of a material. The pressure derivative represents the curvature of the P-V data. Finite-strain theory is used to derive the Birch-Murnaghan EOS, and it is assumed that the material is isotropic and has an elastic response to applied pressure.

The isothermal Vinet, or 'universal' EOS is given by:

$$P_V(V) = 3B_0\eta^{-2/3}\left(1 - \eta^{1/3}\right)\exp\left[\frac{3}{2}\left(B' - 1\right)\left(1 - \eta^{1/3}\right)\right]$$

and is derived from an expression for the cohesive energy of a condensed system. For data collected at high pressures and high temperatures, modified versions of the EOS, incorporating terms that reflect the effects of temperature, must be used instead.

to transform to the face-centred cubic (fcc) structure, between 180 GPa and 790 GPa, depending on which model is used in the calculation [14].

A number of DACs were loaded with high purity magnesium powder together with either tantalum or copper pressure markers. Some DACs were loaded with a methanol:ethanol PTM and some DACs without a PTM.

Room temperature volume compression experiments were performed at two synchrotrons, and ADXRD patterns were collected in incremental pressure steps. After analysis of the data, it was possible to confirm the hcp to bcc phase transformation at approximately 50 GPa.

Figure 11 shows a stacked plot of integrated diffraction patterns. In the lower plot, recorded at 39 GPa, the peaks correspond to reflections from magnesium in the hcp crystal structure. The asterisks indicate unwanted reflections from the rhenium gasket. At 51 GPa (the middle plot) an additional peak appeared between the hcp (002) and hcp (101) peaks. This emerging peak was caused by a reflection from the (110) plane in the bcc structure of magnesium. At a pressure of 83 GPa (the top plot), the sample completely transformed into the bcc phase, showing bcc (110), bcc (200) and bcc (211) peaks. The bcc phase was observed to be stable to at least 225 GPa. There was neither evidence of a complex structure detected above 100 GPa nor evidence supporting a transformation to the predicted fcc phase at 180 GPa.

FIGURE 11

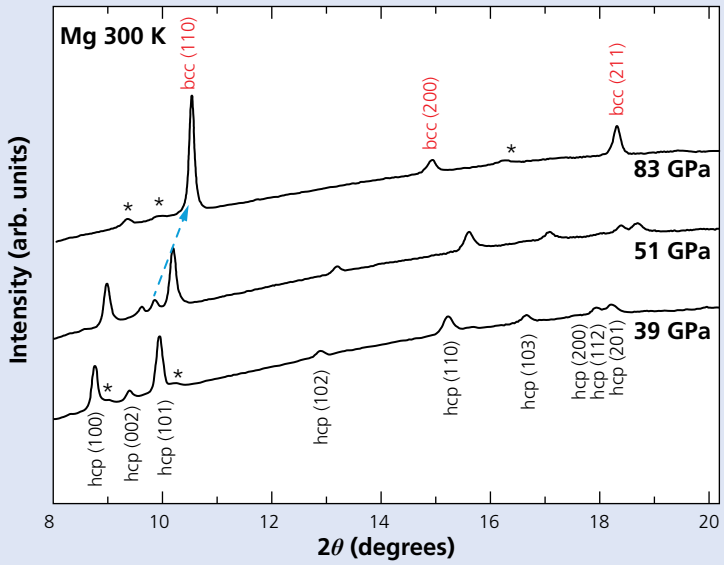

A stacked plot of integrated ADXRD patterns.

The ADXRD pattern corresponding to the integrated pattern at 39 GPa in Figure 11 is shown in Figure 12. Most of the hcp reflections at scattering angles less than 18° are labelled.

A pressure-volume (P-V) plot is shown in Figure 14. These data can be fitted using an EOS to generate values for thermodynamic parameters such as the zero pressure bulk modulus B_0 and its pressure derivative B', as described in Box 2.

FIGURE 12

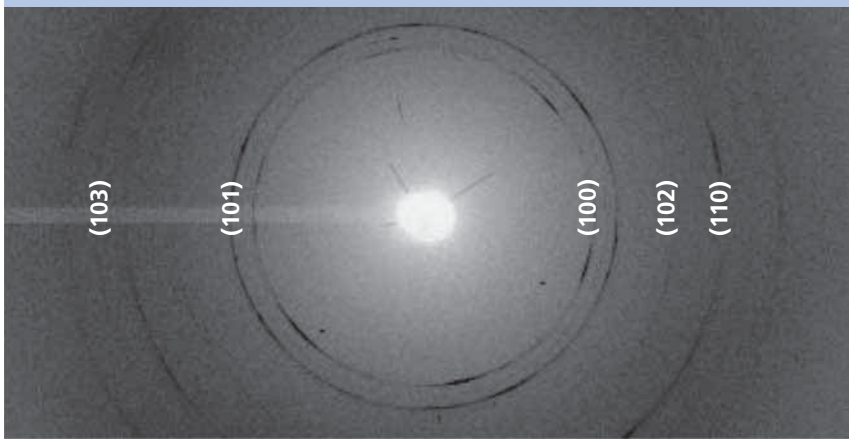

ADXRD pattern collected at 39 GPa.

BOX 3

Synchrotrons

A synchrotron is both a particle accelerator and an electron storage ring. It is a user facility that generates extremely intense and energetic X-ray beams for scientific research. A modern third generation synchrotron typically comprises a linear accelerator (LINAC), a booster, a storage ring, various insertion devices, and at the user end, a number of beamlines that are configured for a particular area of research.

The LINAC accelerates electrons to energies in the MeV range, and these energetic electrons are then injected into the booster ring, which uses bending magnets and radio frequency sources to further accelerate the electrons by three orders of magnitude to GeV energies. Travelling very close to the speed of light, these electrons are then injected into the large storage ring, which employs a complex arrangement of magnets to steer and focus the electrons. The lifetime of the electrons in the storage ring is very long, requiring topping up a couple of times on average a day. Insertion devices use intense magnetic fields to force the electron beam to undulate, producing highly collimated beams of extremely intense X-rays, the wavelength of which can be tuned. Modern third generation synchrotrons can generate X-rays with energies up to 100 keV or more for high pressure experiments. Figure 13 shows the Advanced Photon Source synchrotron, a third generation synchrotron based at Argonne National Laboratory, a US Department of Energy facility near Chicago.

FIGURE 13

Advanced Photon Source synchrotron at Argonne National Laboratory near Chicago.

The EOS fits to the hcp data using the Vinet EOS formulism returning a B_0 value of 33.46 ± 1.13 GPa (i.e. magnesium is very compressible), in agreement with previous measurements. The transition pressure for hcp to bcc was measured to be 50.36 ± 0.12 GPa, also in agreement with previous experiments and predictions [11-14].

Summary

DACs are more than just a piston and cylinder device for the generation of high pressures. The DAC is a versatile tool that is routinely used by researchers to study material properties to millions of atmospheres across many disciplines.

AWE is collaborating with the Institute of Shock Physics at Imperial College London, and with British and international academics, to further knowledge on the response of metals and alloys to extreme pressure.

Acknowledgements

The magnesium experiment was a joint project between AWE, the University of Edinburgh and Lawrence Livermore National Laboratory. The data were collected at the Advanced Photon Source in Chicago and at the Diamond Light Source in the UK.

Use of the Advanced Photon Source was supported by the US Department of Energy, Office of Science.

We thank staff of the High Pressure Collaborative Access Team (HP-CAT) for their support at beamline 16-ID-B.

We thank Diamond Light Source for access to beamline I15 that contributed to the results presented in this article.

Thanks are due to Dr Hyunchae Cynn (LLNL), Dr John Proctor (University of Edinburgh) and Dr Graham Stinton (University of Edinburgh).

FIGURE 14

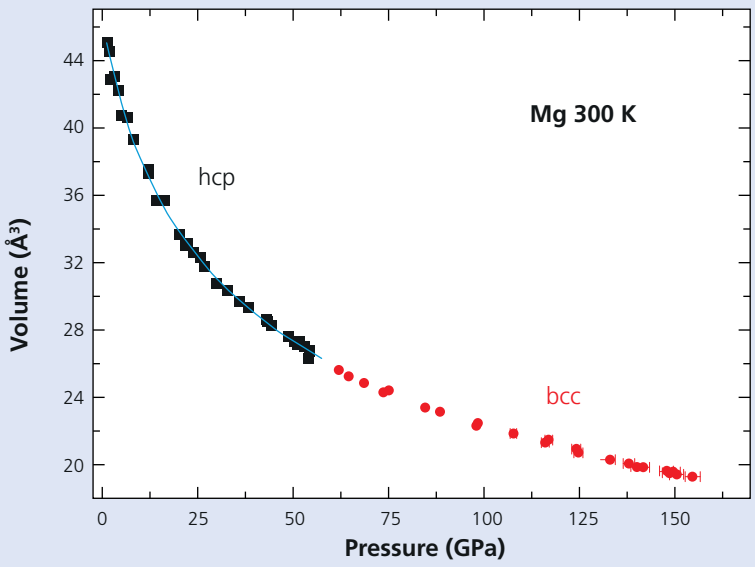

A pressure volume plot showing the transition from hcp to bcc.

References

[1] A. Jayaraman, The diamond anvil high pressure cell, Scientific American 250 (4), 54 (1984).

[2] R.M. Hazen, The diamond makers, Cambridge University Press, Cambridge (1999).

[3] M. Pollington P. Thompson, J. Maw, Equations of State, Discovery, Issue 5, 18 (2002).

[4] P. Taylor, AWE single stage helium gas gun, Discovery, Issue 19, 2 (2009).

[5] A.L. Ruoff, H. Xia, Y. Vohra, Miniaturization techniques for obtaining static pressures comparable to the pressure at the center of the earth: X-ray diffraction at 416 GPa, Rev. Sci. Instrum. 61, 3830 (1990).

[6] M.I. Eremets, I.A. Trojan, P. Gwaze, J. Huth, R. Boehler, V. Blank, The strength of diamond, Appl. Phys. Lett. 87, 141902 (2005).

[7] M.I. Eremets, High pressure experimental methods, Oxford University Press, Oxford (2002).

[8] M.I. McMahon, E. Gregoryanz, L.F. Lundegaard, I. Loa, C. Guillaume, R.J. Nelmes, A.K. Kleppe, M. Amboage, H. Wilhelm, A.P. Jephcoat, Structure of sodium above 100 GPa by single-crystal X-ray diffraction, PNAS 104, 17297 (2007).
[9] E. Gregoryanz, L.F. Lundegaard, M.I. McMahon, C. Guillaume, R.J. Nelmes, M. Mezouar, Structural diversity of sodium, Science 320, 1054 (2008).
[10] H. Fujihisa, Y. Nakamoto, K. Shimizu, T. Yabuuchi, Y. Gotoh, Crystal structures of calcium IV and V under high pressure, Phys. Rev. Lett. 101, 095503, 2208 (2008).
[11] H. Olijnyk, W.B. Holzapfel, High pressure structural phase transition in Mg, Phys. Rev. B 31, 4682 (1985).
[12] H. Olijnyk, Usual broadening and splitting of the k≈0 transverse-optical phonon in hpc Mg at high pressure, J. Phys.: Condens. Matter 11, 6589 (1999).
[13] S. Mehta, G.D. Price, D. Alfè, *Ab initio* thermodynamics and phase diagram of solid magnesium: a comparison of the LDA and GGA, J. Chem. Phys. 125, 194507 (2006).
[14] A.K. McMahan, J.A. Moriarty, Structural phase stability in third-period simple metals, Phys. Rev. B 27, 3235 (1983).

AUTHOR PROFILE

Simon Macleod
Simon joined the Hydrodynamics Department at AWE in 2005 and was initially responsible for developing optical pyrometry as a shock temperature diagnostic. Since 2007 Simon has been responsible for developing the diamond anvil cell capability. Simon is now in the Design Physics Department and holds a visiting research fellowship at the Institute of Shock Physics at Imperial College. He collaborates with the Centre for Science at Extreme Conditions (CSEC) at the University of Edinburgh and with Lawrence Livermore National Laboratory.

AUTHOR PROFILE

Malcolm McMahon
Malcolm is Professor of High Pressure Physics in the School of Physics and Astronomy at the University of Edinburgh. He is Deputy Director of the University's Centre for Science at Extreme Conditions, and since October 2011, holds a William Penney Fellowship at AWE. Malcolm's research interests are in using X-ray diffraction to uncover the behaviour of simple materials (elements and simple molecular systems) to extreme pressures. He is a frequent user of synchrotron sources in the UK, Europe and the US, where he has developed techniques to collect and analyse diffraction data from both polycrystalline and single crystal samples. Most recently, his research interests have moved to the use of dynamic compression techniques to push structural studies of matter well beyond the current limits of DACs.

High Current Pulsed Power

material testing using AMPERE

High current pulsed power is a means of dynamic material testing which has not been exploited at AWE for more than 20 years. In the intervening period, high explosives and gas guns have been the standard tools with which to drive materials to extremely compressed states and high strain rates in order to test their response. The Equation of State (EOS), material strength and other data resulting from these types of experiments remain vital for the continuing improvement of the computer models that lie at the heart of AWE's Design Physics capability. The electromagnetic forces caused by high currents can be larger, more controllable, faster and less hazardous than these other methods and are consequently utilised in many laboratories around the world for civilian and defence research.

The work described here represents the recent efforts by AWE to re-establish its electromagnetically driven high energy materials research. The first facility, called AMPERE, was commissioned by AWE and is now fully operational and ready to perform its first series of trials. The machine was given its name in honour of André-Marie Ampère, the famous French scientist who first discovered electromagnetic force.

The primary function of the AMPERE pulsed power generator is to drive coupon scale foil slap trials. No other facility in the UK or US is currently able to perform this type of testing with electromagnetic propulsion. Foils and metal plates colliding with a target are considered to be an effective method of producing a large, rapidly rising pressure impulse and are the most accurate method of simulating shocks resulting from exposure to cold X-rays.

The effects created by a shock wave in a material are typically monitored by observing the motion and any spalling of the rear surface. The target ablation and simulation are depicted in Figure 1.

Foil slap trials consistently create appropriate simulation pressure pulses onto the front surface of a target, but do not require a large X-ray source. Of most importance, this technique can generate the magnitude and time profile of the mechanical pressure impulse simultaneously over large surface areas and can therefore be used to robustly test continuum or composite materials.

AMPERE has been designed in the first instance to investigate coupon sized sections of flat and curved composite materials. The impact area of the coupon scale targets is many 10s of cm^2 which is essential to discern any effects due to the anisotropic nature of certain composite structures.

The entirely in-house development of AMPERE has dramatically

FIGURE 1

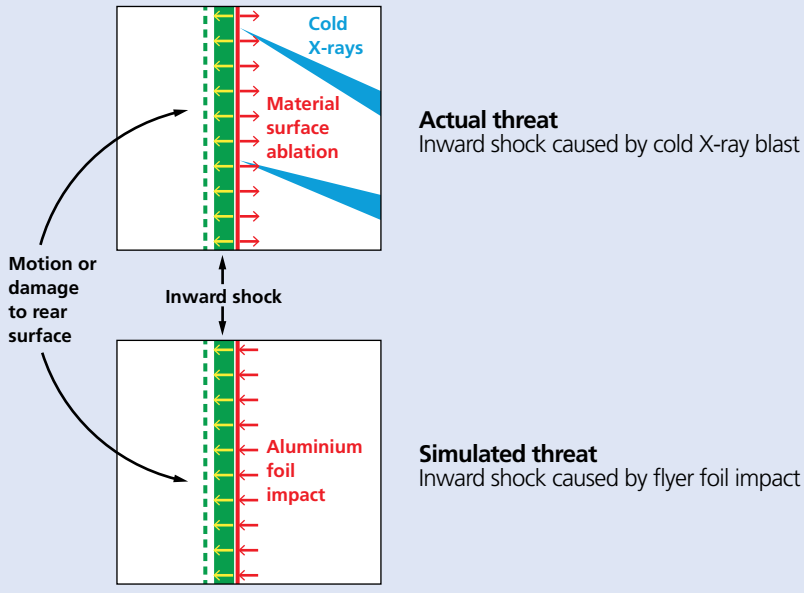

Depiction of target ablation by X-ray and simulation by impact.

improved AWE's capability to design and field high current pulsed power systems for foil slap and other dynamic material testing applications in a timely and cost effective manner.

AMPERE has provided a convenient test bed with which to trial crucial foil and target preparation techniques. Early coupon scale experiments have allowed experience to be gained with the optical interferometric velocimetry diagnostics, developed at AWE, specifically for X-ray induced impulse measurements [1], which are required to measure the target response.

Foil slap – historical precedents

Electromagnetically driven foil slap testing was previously deployed by the US Air Force during the 1960s-80s. During the late 1970s-80s, a very large foil slap programme at AWE developed the GRIMM capacitor bank [2], shown in Figure 2, which was capable of accelerating thin foils with areas up to 1.4 m^2.

These trials also included accelerating complex geometry foils to impact shaped targets. A similar test rig was developed by

FIGURE 2

GRIMM capacitor bank.

ITT and Defense Threat Reduction Agency (DTRA) in the US during the 1990s and early 2000s. The diagnostics for these trials were primarily piezoresistive carbon gauges and time of arrival (TOA) probes.

Both techniques suffered from being intrusive to the target and difficult to field in the electrically noisy environment of a high current discharge.

Other foil acceleration techniques have been used for cold X-ray simulation in the past and some are still actively being developed to produce similar results. At Sandia National Laboratories (SNL) a technique called the X-flyer has been developed in which light initiated high explosive (LIHE) is used to launch a foil flyer plate into the target. This explosive is applied to the foil as a liquid and when dried can be detonated by a bank of pulse power driven flash lamps.

The highest velocity and pressure foil slap tests are currently being performed on the Z accelerator at SNL [3]. Although the foils are small (25 mm x 13 mm), they pass currents of up to 20 MA and acquire velocities up to 45 kms^{-1} resulting in multi-megabar pressure on targets of interest.

In this regime, one of the major technical challenges is preventing all of the flyer foil from melting so that some solid metal strikes the target. This is achieved by very careful current pulse shaping to

"A pulse with a longer rise time will spread more evenly throughout the conductors and thus the acceleration on all parts of the foil will be more uniform."

avoid any shock heating within the flyer prior to target impact.

AMPERE experimental equipment

AMPERE is a high current pulsed power generator consisting of 12 capacitors, connected in parallel and discharged through a single triggered rail gap switch into a two component strip line load [4].

These two devices, namely the foil flyer assembly and exploding foil dynamic resistor (EFDR), will be discussed separately. The capacitor bank can be charged to 40 kV. Since no higher voltages are impressed on any of the conductors, none of the components need to be immersed in transformer oil.

The pressurised switch has been calibrated to perform with a gas mixture of argon and oxygen. This removes the need to use sulphur hexafluoride, which is the traditional high voltage switching medium, but is also a polluting greenhouse gas controlled by the Montreal Protocol.

The bank can store up to 123 kJ of energy and produce 'long' current pulses of more than 600 kA, lasting 10s of microseconds.

The system is protected by three automated independent dumping systems and several monitoring devices and CCTV surveillance. The capacitor bank and optical table which supports the two loads are enclosed in an interlocked security cage and all systems are controlled by operators in a remote screened room. Figure 3 shows the AMPERE system.

The AMPERE electric circuit is a simple LCR configuration in which the rise time of the current is determined by the physical layout and the maximum current is a function of the voltage to which the capacitor bank is initially charged.

FIGURE 3

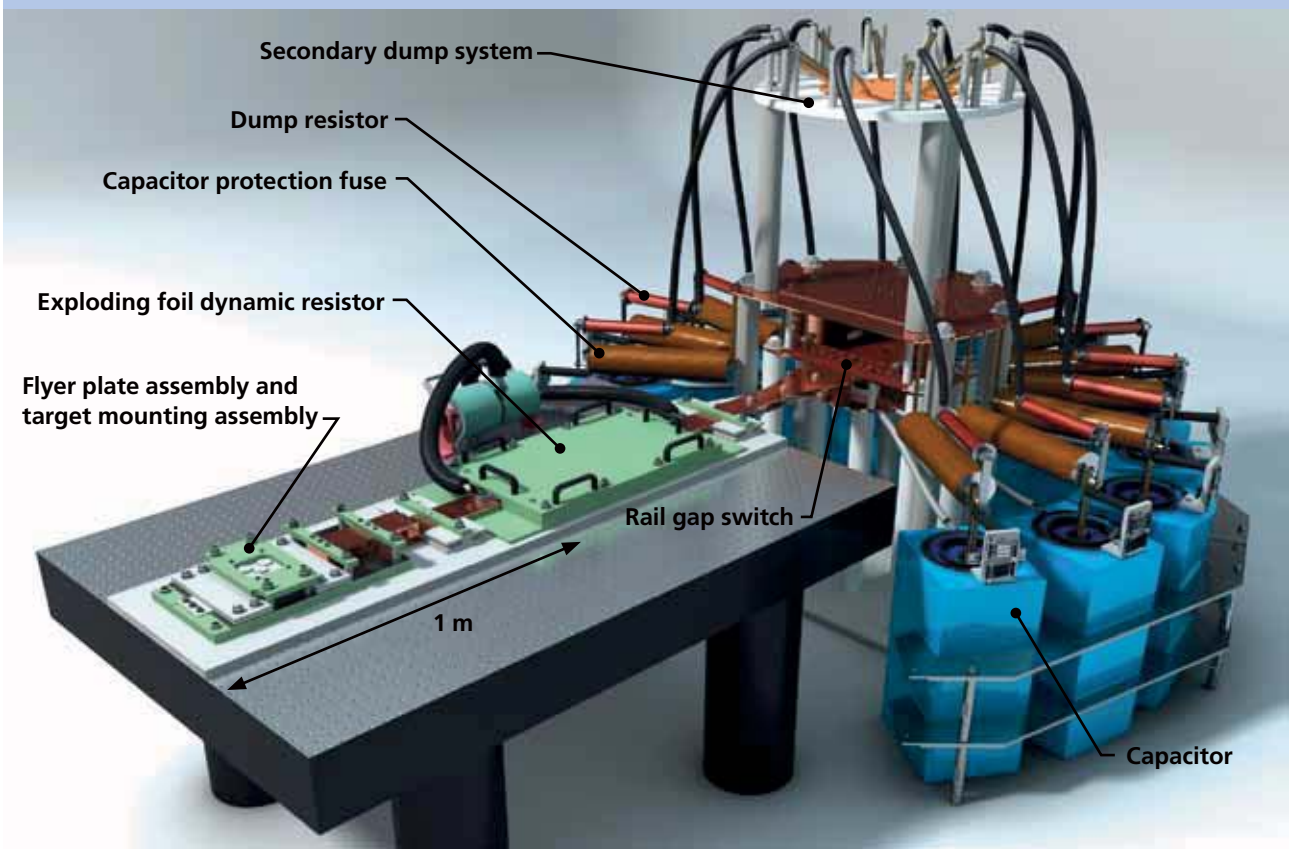

AMPERE pulsed power generator.

FIGURE 4

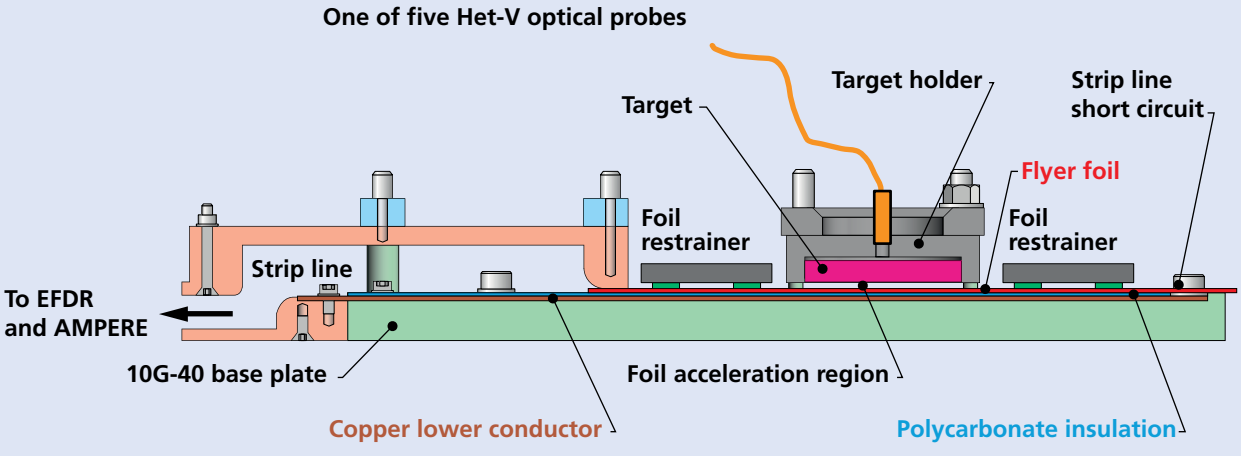

AMPERE foil flyer assembly (section along centre line).

The overall inductance of the capacitor bank has not been radically minimised as is done in most pulsed power applications since there is an advantage to having slower pulses when accelerating large foils. This is energetically expensive, but affordable for coupon scale testing.

A pulse with a longer rise time will spread more evenly throughout the conductors and thus the acceleration on all parts of the foil will be more uniform. This enhances the simultaneity requirement of impacting all regions of the target at the same time which is very important when simulating a single source X-ray exposure.

Foil flyer assembly

The flat coupon scale target is initially lightly supported in a nylon holder a few millimetres above a metal flyer foil. This thin foil is a section of the upper conductor of a strip line configuration as seen in the center line section shown in Figure 4. The actual foil flyer assembly is shown in Figures 5 to 7. The foil is several centimetres in width and is stretched and held between two fixtures.

There is a short circuit at one end where the flyer foil is electrically and mechanically clamped to the lower copper line. At the other end the foil is held firmly between the large copper upper conductor and the 2 mm polycarbonate

FIGURE 5

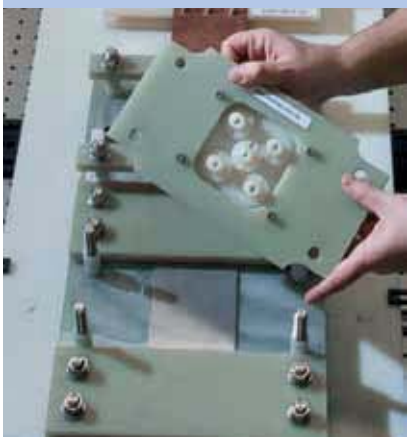

Foil flyer assembly – target holder removed.

FIGURE 6

Foil flyer assembly – target holder in position.

insulation that separates it from the lower line. The section of the lower conductor that lies under the flyer foil is the same width as the foil and set into a slot, milled into a dielectric 10G-40 base plate, which restrains it and adds inertial mass.

The target initially rests above the centre of the foil and symmetrically between both clamped ends. The time required for the foil to cross the foil acceleration region between its initial position and the target is so short, that this central region of the foil does not have time to feel the effect of the clamped ends prior to impact. This is very useful because it allows the foil to be stretched when it is mounted, thus ensuring that its initial form is highly planar which improves the likelihood of simultaneous impact across the whole target.

The outer sections of the flyer foil are impeded by restrainers mounted slightly higher than the target so that they do not interfere with the target impact being observed.

The target holder is also designed to mount five optical probe heads arranged as the five spots on a die. These can be adjusted so that the laser light can be accurately focused on the rear surface of the target.

In addition, by using transparent LEXAN targets, the probes can also either be focused on the initial position of the flyer foil to measure its velocity as it approaches and rebounds from the target or on the front surface of the target to measure its motion and thus deduce the applied pressure pulse.

FIGURE 7

Foil flyer assembly – post firing.

Exploding fuse dynamic resistor (EFDR)

Due to the usual distribution of inductance and resistance in an LCR circuit, a normal capacitor discharge through a low impedance load yields a damped ringing discharge, with multiple positive and negative voltage and current peaks of decaying magnitude.

This type of discharge has two disadvantages for the AMPERE foil slap programme. Firstly, the rapid reversal of high voltage across the dielectric within each capacitor causes microscopic damage and decreases their overall lifetime and performance. Secondly there is another drawback to the ringing discharge which is that the flyer foil is accelerated during the current peaks and not during the current zero crossings. This means that the flyer foil receives a series of accelerating impulses rather than a single push. During the coasting phases, the foil will be

more susceptible to fluctuations in pressure between the foil and target and therefore there is more chance of divergence from planarity. AMPERE was designed so that the foil received only a single acceleration pulse which would last up to and slightly after the target impact. Any further current peaks would also lead to repeated high force impacts on the target. Since some of the targets will be taken away after the foil slap to investigate long term damage, these re-strikes are not desirable.

Both problems were removed, by introducing a current pulse shaping component into the circuit which allows one large current peak to pass and then quenches all further peaks. Comparison between ringing and fuse commutated discharge is shown in Figure 8.

This pulse shaping is achieved by including a very accurately tailored fuse into the circuit. In AMPERE, this is achieved by exploding a 50 µm thick aluminium foil. Its length is fixed, but its width is very carefully selected to match the specific shot parameters, namely capacitance, initial charging voltage and circuit geometry.

After the gas switch is triggered, the current builds up in both the flyer foil and the exploding foil fuse. Since the fuse foil is much thinner than the flyer foil, it has more electrical resistance and heats up faster. This runs quickly to the temperature at which the metal bursts explosively and goes 'open circuit'.

The initial dimensions of the foil are carefully selected to ensure that the foil explosion occurs very near the first current zero crossing.

FIGURE 8

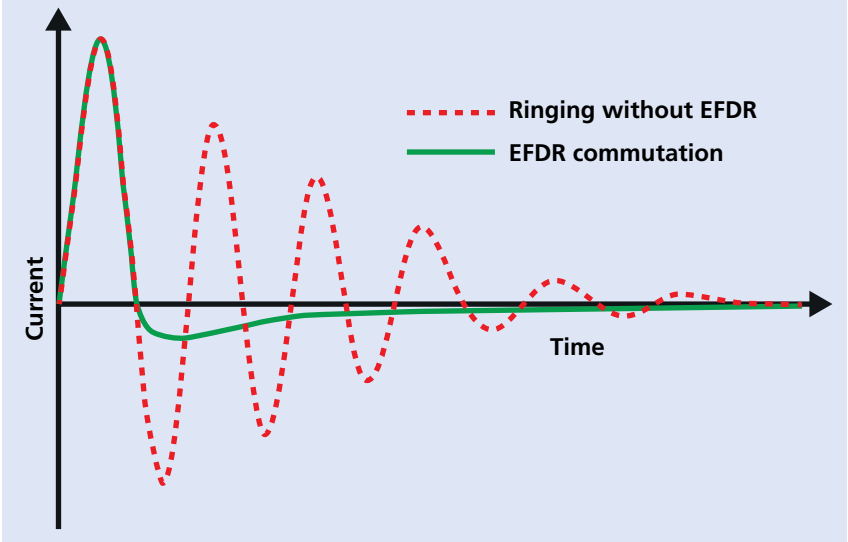

Comparison between ringing and EFDR commutated discharge.

This minimizes the rate of change of current at the fuse explosion to reduce induced voltage spikes at vulnerable points in the circuit. A large ceramic resistor is connected to the circuit in parallel with the exploding foil which slowly absorbs all of the remaining energy in the circuit after the fuse has blown which has the effect of severely damping the rest of the current pulse. This technique has proved to be very reliable and makes the AMPERE foil slap facility the first one that can avoid strong target restrikes.

To contain the explosion, the 50 µm exploding foil is laminated between two layers of 250 µm thick Mylar and this composite is buried in the middle of an enclosed box of dry sand. The lid of the 10G-40 dielectric sand box is held down with strong springs that allow venting of the explosion overpressure, but close again quickly to minimize the amount of sand that is ejected.

Most of the molten metal remains contained within the Mylar lamination and most of the sand remains uncontaminated and can be reused between shots. A foil, photographed before and after an explosion is shown in Figure 9 and 10 respectively.

Heterodyne velocimetry (Het-V) diagnostics

Measurement of flyer foil velocity, as well as motion of the front and back surfaces of LEXAN targets, has been performed using Het-V probes fielded by AWE. Three different interferometric

techniques have been utilised, but conveniently all of them use the same optical fibres and lenses to bring the data from the target holder to the screened room. Switching between techniques therefore does not involve any changes in the AMPERE experimental enclosure.

Exploiting the transparency of the LEXAN target, the Photonic Doppler Velocimetry (PDV) and Frequency Shifted Photonic Doppler Velocimetry (FS-PDV) techniques were used to measure the foil velocity [1,5].

Both methods involve splitting a signal from a laser and using one fibre as a reference. The other fibre is sent to the experiment where the frequency is Doppler shifted after reflecting off a moving surface. When the two beams are recombined, the signal is recorded on a single oscilloscope channel and the resulting beat frequency is proportional to foil velocity.

In the case of the FS-PDV, the signal in one of the fibres is shifted by 500 MHz, which places a 320 ms^{-1} velocity offset into the analysis. When this velocity is later subtracted, the result is an unambiguous measurement of direction as well as velocity which is very useful when observing the foil reversal at target impact. This technique is relatively coarse, but well suited for velocity measurements over several millimetres.

A third and significantly more sophisticated technique called Photonic Displacement Interferometry was employed for more accurately monitoring the much smaller displacements of the front and rear surfaces of the target [6]. It differs from the previous two methods by employing a 3 by 3 splitter where the two beams are recombined. It introduces a $2\pi/3$ phase shift into three versions of the normal beat frequency output. Consequently, this requires 3 oscilloscope channels per single velocimetry probe, however it leads to a more precise velocity and displacement measurement. Resolution down to 15 nm is possible.

In order to obtain a strong reflected signal from the target surface, pieces of very thin aluminium were carefully glued to the surface under observation. For future trials on LEXAN and composite materials, a very

FIGURE 9

EFDR fuse before explosion.

FIGURE 10

EFDR fuse after explosion.

thin layer of aluminium will be vacuum deposited on the surface for higher accuracy.

AMPERE – modelling

AMPERE and the coupon scale foil slap trials were originally designed using an IDL code now called AMPFLY, specifically written for this experimental programme. It is a 1D analysis that predicts the current pulse and foil acceleration from a set of initial conditions.

It has proved to be reliable because the AMPERE generator, EFDR and foil flyer have all performed very closely to the predictions made prior to construction and testing [6]. It was realised at an early stage that AMPFLY would not be sufficient to design a flyer foil assembly capable of performing foil slap tests on curved targets. Therefore a multi-pronged modelling strategy was implemented.

AWE has been studying the applicability of some higher dimensional codes from the US, namely ALEGRA and MULTIFLY. AWE is also collaborating with Loughborough University to investigate 2D filamentary modelling of the flyer foil [7]. In addition, a separate 1D circuit model was developed using MATHCAD software called EMSLAP and used to validate the AMPFLY predictions.

In all of the models, the flyer foil is considered to be accelerated by electromagnetic force due to repulsion from the stationary lower conductor. The foil deceleration is modelled as a 1D adiabatic gas compression of the air between the foil and the target (i.e. the gas is assumed to not escape sideways or heat up).

Currently, all of the models are roughly agreeing with each other, but are all over predicting the acceleration and maximum flyer foil velocity by up to 10%. This error was also experienced by DTRA staff who developed their own foil slap models. It seems likely to be due to the inability to consider subtle perturbations in the flyer-gas-target interactions without a full 3D model.

Nevertheless, since a consistent level of over prediction can be ascertained, this correction will be incorporated into future models used to design more complex foil slap configurations.

Foil slap experimental campaign

The initial experiments on AMPERE were performed to gain more refined knowledge of the behaviour of the EFDR. In these tests, the flyer foil was replaced by a static 2 mm thick stainless steel plate. Experiments with narrower EFDR aluminium foils could be compared to data in the published literature to build up a more accurate understanding of the relationship between aluminium resistivity as a function of deposited energy density.

It is now well known that this relationship is not only a property of the metal itself, but is significantly affected by both the rate of rise of the current pulse and also the mechanical environment surrounding the foil.

The form of the resistivity curve required by a computer model is thus very specific for a particular experimental arrangement. Nevertheless, low energy foil explosions could be used to gain confidence in the model prior to designing EFDR foils for higher energy discharges.

An empirical resistivity curve has now been derived which reasonably fits the entire range of anticipated coupon scale foil slap experiments.

The second series of tests involved the flyer foil impacting LEXAN targets. This allowed the Het-V probes, operating in the FS-PDV mode to look through the target and measure the foil velocity at five locations from stationary to maximum upward acceleration, to deceleration approaching the target and finally both rebounding from the target and striking the bottom insulator again.

Integration of this velocity curve yielded the upward and downward foil displacement which always agreed with each other for any single probe, demonstrating the very high accuracy of this diagnostic technique. It revealed that on many occasions the distance travelled by different sections of the foil were not always equal as shown in Figure 11. The earliest discrepancies were up to ± 200 µm in a total travel of 2 mm, leading to an unsatisfactory loss of impact

simultaneity. This was considered to be a result of imprecise initial setup.

Consequently, new techniques including pre-stretching the flyer foil, stiffening several structures and using new measurement devices reduced these errors to within acceptable limits. These tests were performed to confirm the applicability of the AMPFLY computer model that calculates the current pulse and flyer foil motion up to the point of target impact as long as the acceleration was reduced by the 10% 3D correction factor.

Employing a division of tasks between the five probe locations, this series of low energy discharges allowed measurement of the motion of both the front and back surfaces of the LEXAN target as well as the flyer foil velocity all on the same shot. This allowed the experimental relationship between flyer foil velocity and applied pressure pulse to be compared with values predicted by hydrocodes such as ALEGRA.

The latest experiments on AMPERE were designed to better control the magnitude, rise time and simultaneity of the pressure pulse applied to the LEXAN target. Demonstration of improved planar target impact is shown in Figure 12.

Controlling the magnitude and rise time of the pressure pulse applied to the target was achieved by varying the maximum flyer foil velocity as well as the initial foil to target gap length which determines the number of gas molecules to be compressed. The aim was to use gap lengths and foil velocities which the ALEGRA model had determined would produce predictable and useful pressure impulses on composite material. These recently reported tests were very successful and have laid the groundwork for upcoming composite material cold X-ray impulse simulation trials.

FIGURE 11

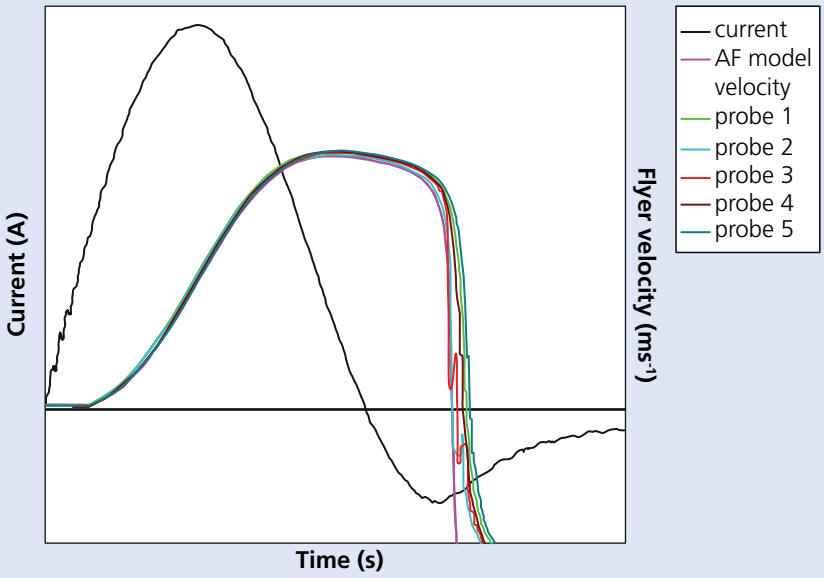

Current and foil velocity.

FIGURE 12

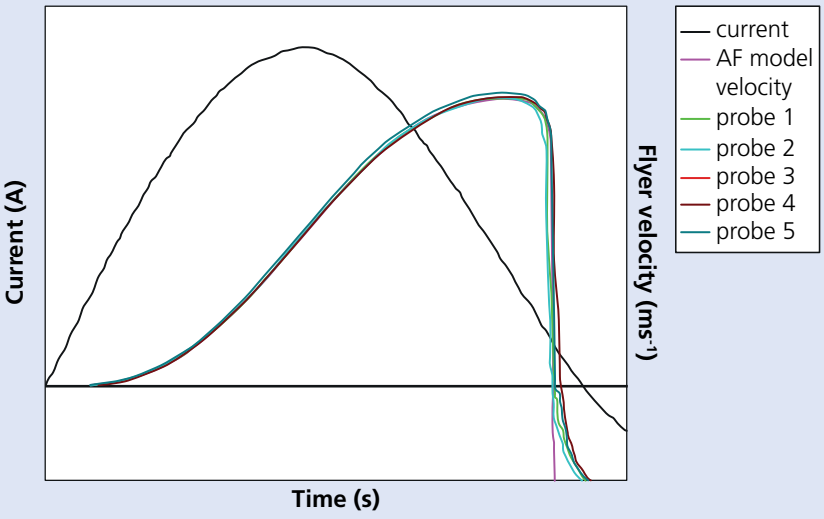

Current and foil velocity – improved planar target impact.

"AMPERE was designed to be a versatile facility, capable of driving a range of dynamic material testing experiments that previously relied on high explosives or gas guns."

Future developments

AMPERE was designed to be a versatile facility, capable of driving a range of dynamic material testing experiments that previously relied on high explosives or gas guns.

The first of these tests is already past the design review stage and will soon be constructed. It aims to drive a high current pulse through a solenoid which is mounted inside a metallic cylinder which is the test material as shown in Figure 13.

The current in the solenoid induces currents in the test cylinder and the net electromagnetic forces cause its rapid radial expansion. High speed photographic observation of the cracking and breaking up of the cylinder, under high strain rate, will yield valuable ductility data for a variety of materials.

FIGURE 13

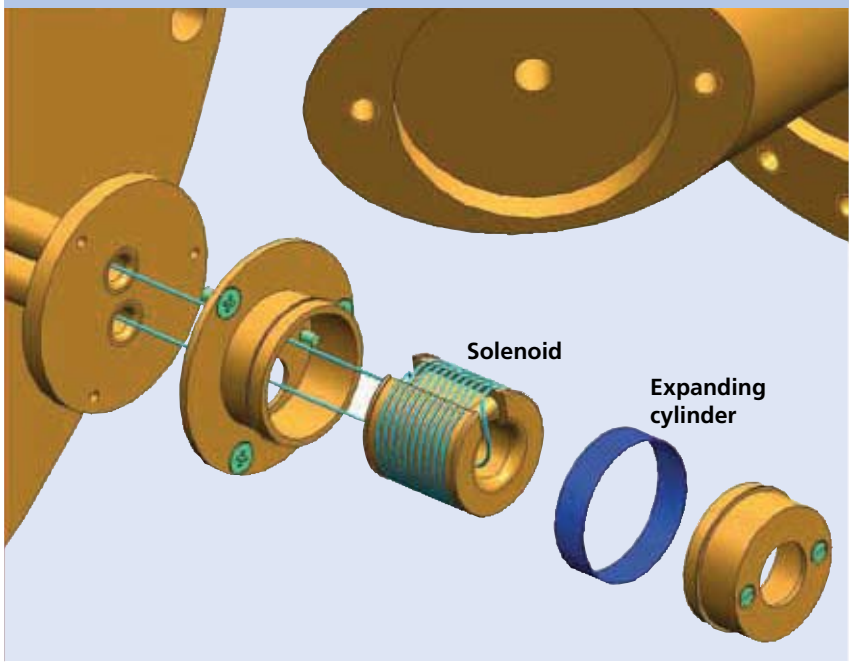

Exploded view of a solenoid mounted inside a metallic cylinder.

It is expected that the coupon scale foil slap programme will need to be an ongoing capability at AWE as novel pure and composite materials continue to be developed and will need validating against a perceived cold X-ray threat.

The AMPERE facility has been designed to be versatile and provide many years of service. AMPERE is perfect to test innovative ideas such as multiple switching for pulse shaping or different cabling techniques which will be needed if it is decided that a larger high current pulsed power generator is required at AWE.

Such a machine would have strategic application as a very high pulsed magnetic field source which is of interest both to material scientists as well as biologists and other scientists.

At the moment, the long term goals of such a development programme are to obtain an in house isentropic compression experiment (ICE) capability and or a large scale foil slap X-ray simulator.

The many benefits of high current pulsed power such as low hazard, large force, rapid rise time, predictability, repeatability and reliability mean that such machines will most likely play major roles in the future of AWE. AMPERE will not only provide some very important data in both the short and long term, but will

be an excellent learning tool for taking the first steps down this path.

References

[1] A. Sibley, A. Hughes, Photonic displacement interferometer, Discovery Issue 21, 2 (2010).

[2] R. Bealing, P.G. Carpenter, Efficient magnetic flier plate propulsion, J. Phys. D: Appl. Phys. 9, 151 (1976).

[3] R.W. Lemke *et al.*, Magnetically driven hyper-velocity launch capability at the Sandia Z accelerator, Int. J. Imp. Eng. 38, Issue 6, 480 (2010).

[4] N. Graneau, K. Omar, Development of a pulsed high current facility for accelerating metal foils for hydrodynamic materials testing, Acta Physica Polonica A 115 (6), 1086 (2009).

[5] O.T. Strand, D.R. Goosman, C. Martinez, T.L. Whitworth, T.W. Kuhlow, Compact system for high-speed velocimetry using heterodyne techniques, Rev. Sci. Instrum, 77, 083108 (2006).

[6] D.H. Dolan, S.C. Jones, Push-pull analysis of photonic doppler velocimetry measurements, Rev. Sci. Instrum. 78, 076102 (2007).

[7] B.M. Novac, K. Omar, N. Graneau, I.R. Smith, M. Sinclair, Numerical modelling of a foil-flyer electromagnetic accelerator, 18th IEEE Pulsed Power Conference, Chicago, USA (June 2011).

AUTHOR PROFILE

Neal Graneau

Neal Graneau received a BSc degree in Physics from King's College London University in 1986 and a MSc and D.Phil degrees in Plasma Physics from the University of Oxford in 1987 and 1992 respectively. His research interests span from experiments in fundamental electromagnetism and their implication in matter interaction theories to renewable energy devices exploiting the electrical manipulation of liquids.

Neal is currently a senior scientist in the Pulsed Power Design Team in the Hydrodynamics Department at AWE, leading the development of high current pulsed power machines for dynamic material properties research.

AUTHOR PROFILE

Kaashif Omar

Kaashif Omar graduated from the University of Leicester with a MPhys in Physics with Astrophysics in 2007. His early research interest in carbon nanotubes has now led to high current pulsed power and electromagnetic mass accelerators. He has been responsible for the project management of the development and running of AMPERE in addition to design, construction and other technical roles in the programme. He has written a 1D code which is capable of accurately predicting the electrical and mechanical performance of the AMPERE facility and is working closely with Loughborough University on a part time PhD to design and test various methods and sensors to assist the further development of this type of technology.

Nuclear Data for Neutronic Systems Modelling

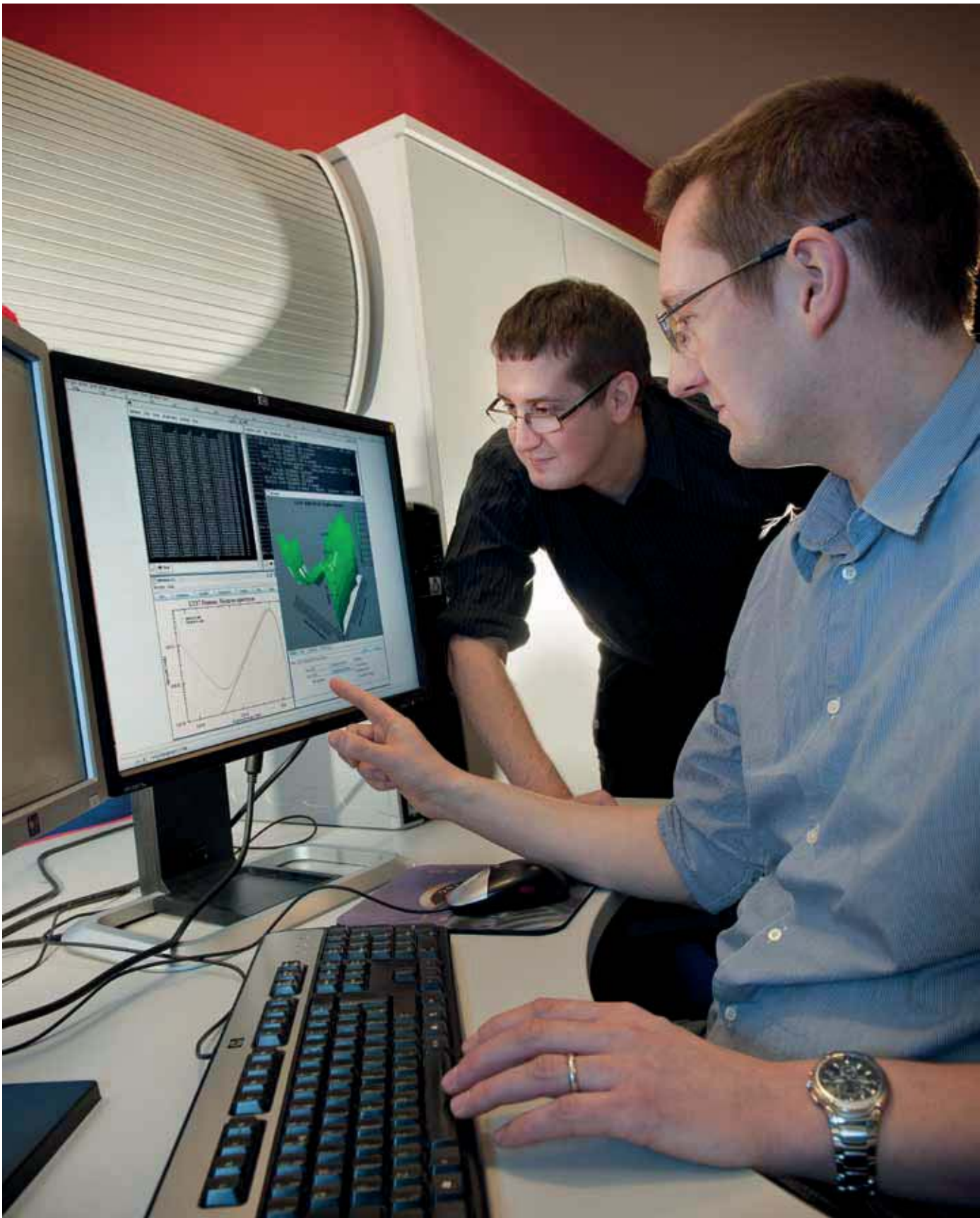

Reliable nuclear data are an essential component of the physics based modelling of neutronic systems. The principal responsibility of the Nuclear Data Team is to provide data suitable for use with AWE's modelling codes.

The term nuclear data, although associated with any intrinsic properties of nuclei, is used in the current context to apply specifically to the interaction of neutrons with nuclei, the consequent reaction type and resulting products.

Neutron cross-sections

A fundamental concept for any consideration of particle interaction with matter is the cross-section, which is an expression of the likelihood that a reaction will take place. In the classical limit of an effectively zero sized particle interacting with a nucleus, the likelihood of interaction is represented by the cross-sectional area of the nucleus, πR^2 where R is the nuclear radius. The correct quantum mechanical description of the process is however, much more complex and the cross-section can be many orders of magnitude greater or smaller than πR^2. The total interaction cross-section is the sum of a number of partial cross-sections as described in Box 1.

The distinctive nature of the neutron-induced fission cross-section of plutonium-239 (^{239}Pu) is shown in Figure 1. At thermal energies the cross-section shows the normal $1/v$ behaviour for reaction cross-sections, where v is the neutron velocity. In the energy range of a few electron volts (eV) to several kilo electron volts (keV), the cross-section displays a resonant structure where the energy available to the absorbed neutron coincides with energy levels of the compound neutron-plus-nucleus system. This reaction mechanism persists into the unresolved resonance region but here the levels of the compound system are either too finely spaced to show distinct structure, or are unable to be resolved experimentally. In the fast region the resonance structure has disappeared and only slowly varying gross features are apparent.

Neutron cross-sections are used by neutronics modelling codes principally to solve the Boltzmann transport equation for the system angular neutron flux, as described in Box 2. This flux solution can be obtained either by Monte Carlo methods, where individual neutrons are tracked through the

FIGURE 1

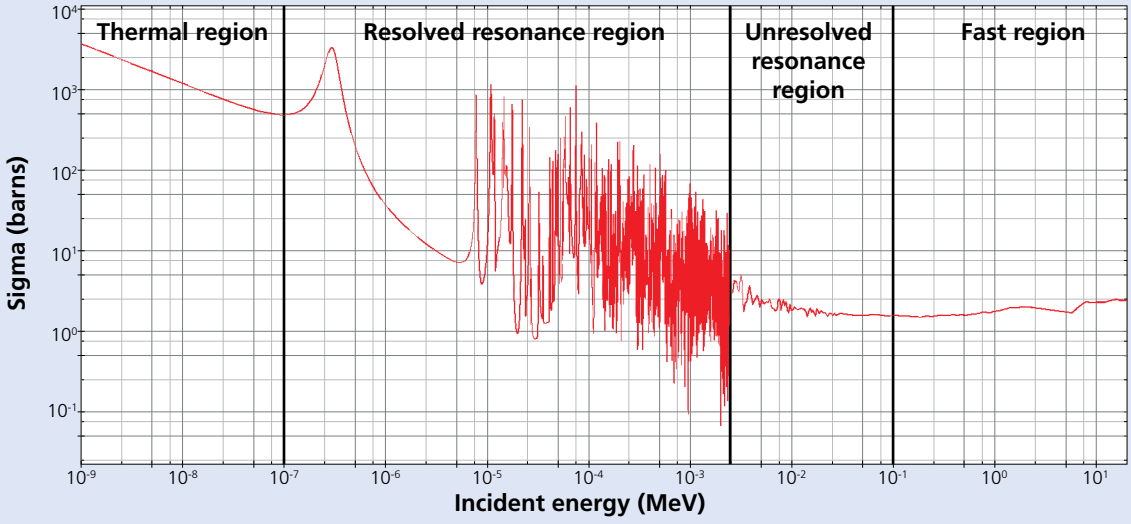

The evaluated neutron-induced fission cross-section of ^{239}Pu, plotted logarithmically, from thermal energies up to 20 MeV (million electron volts). The energy boundaries of the regions defined in the figure are normally set by the evaluator.

BOX 1

Neutron interaction cross-sections

The likelihood that an incident neutron will react with a target nucleus is described by the 'total' cross-section and is denoted σ(total). In the following expression the total cross-section is represented as the sum of 'partial' cross-sections, each one of which represents the likelihood of a specific reaction:

$$\sigma(\text{total}) = \sigma(\text{elastic}) + \sigma(\text{gamma}) + [\,\sigma(\text{inelastic}) + \sigma(\text{neutrons}) + \sigma(\text{fission}) + \text{other cross-sections}]$$

where the partial cross-sections are:

- σ(elastic) = elastic scattering (1 neutron emitted)
- σ(gamma) = capture reaction (gamma ray emission)
- σ(inelastic) = inelastic scattering (1 neutron + gamma ray emission)
- σ(neutrons) = more than 1 neutron + gamma ray emission
- σ(fission) = fission reaction (neutrons + fission products + gamma rays)

The elastic and capture reactions are always energetically possible, however the cross-sections enclosed in the square brackets denote that the reaction will only take place if the incoming neutron is above a certain threshold energy. In addition, the fission reaction will clearly only occur if the nucleus is *fissionable*; nuclides such as ^{235}U have a zero threshold for fission and are termed *fissile*. A set of cross-sections for neutrons interacting with ^{235}U is shown in Figure 2.

FIGURE 2

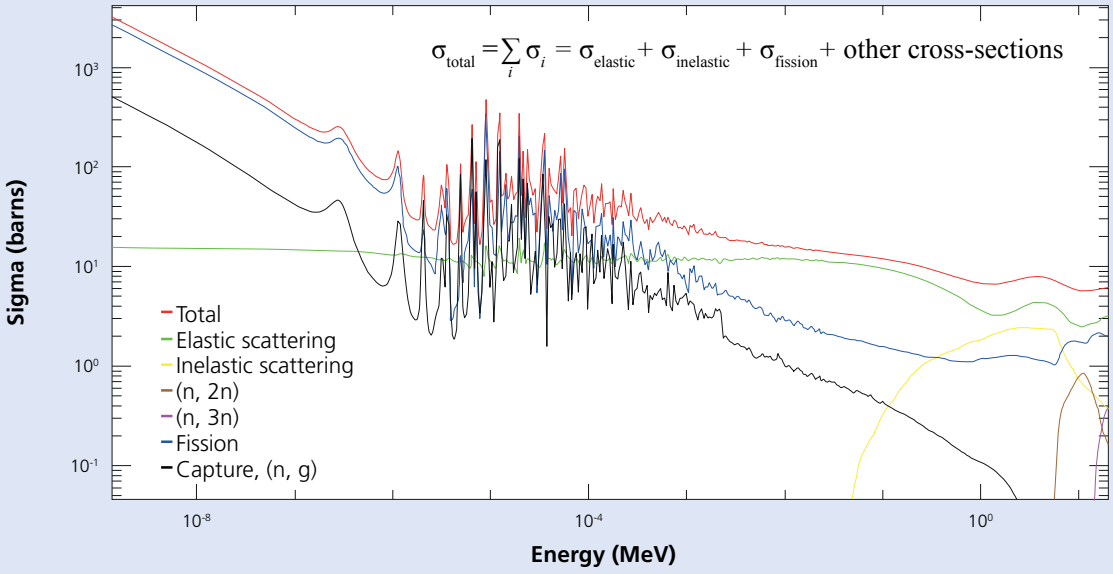

The total cross-section and partial cross-sections of ^{235}U from thermal energies to 20 MeV. Cross-sections have units of area and are measured in barns, where 1 barn = 10^{-24} cm^2.

system under study and their interaction histories recorded, or by discretising in time, energy, space and angle and solving the transport equation iteratively, as a deterministic problem.

Data sources

Cross-section data are collated and evaluated at a network of 14 data centres worldwide. Physicists at these centres assess the available data for a nuclide, derived from experiment and/or theory, and produce a recommended set of data. This evaluation is a subjective process, hence evaluations differ from centre to centre.

The three major evaluation projects are: JEFF (Joint Evaluated Fission and Fusion) based in Europe, ENDF (Evaluated Nuclear Data File) based in the US and JENDL, the Japanese Evaluated Nuclear Data Library.

NJOY processing

Nuclear data in its evaluated form cannot easily be used directly; processing into a friendlier and more accessible form is therefore required. The NJOY code is an internationally recognised standard [1] for undertaking this task; data can be cast into both continuous format for Monte Carlo applications, or group format for deterministic code applications.

Using NJOY requires specialised knowledge and skills. In recent years Serco Assurance have performed the necessary data processing for AWE, delivering data for a wide range of nuclides from the most up-to-date JEFF, ENDF and JENDL evaluations. These data are in a specialised group format called GENDF (Group ENDF), on a high fidelity 460 energy group grid.

Data validation

The GENDF files must be checked and validated by the Nuclear Data Team to ensure the data are fit for purpose; this validation is performed through application of a code called NDval (see Box 3). The data are then converted to AWE's format and benchmarked against standard systems. These take the form of critical assemblies and device models chosen from standard benchmark suites. If the data adequately reproduce the expected results – experimental values in the case of critical assemblies and previous calculations in the case of device models – then they are considered acceptable for use in modelling codes.

Data adjustment and comprehensive libraries

Constraints imposed by calculation time and memory usage mean that fine group data are rarely used in mainstream calculations; consequently, a set of production libraries must be created in a range of coarse group structures. For example, one dimensional (1D) models would generally be calculated using a standard 105 group structure, whereas for 3D models, 32 groups or fewer would be more appropriate.

Data adjustment is required to compensate for loss of accuracy when group structures are coarsened or when approximations are applied in neutronics transport algorithms; libraries are therefore produced in a variety of combinations of group structures and transport approximations. The data adjusted are the principal partial cross-sections of the nuclides ^{239}Pu, ^{235}U and ^{238}U. The adjustment procedure uses the AWE code NDxadj to vary selected cross-sections in broad energy regions such that a best fit is obtained to a set of standard benchmark systems.

To produce the final working or comprehensive libraries the code NDLI is used to apply any adjustments, condense the data and add specialised cross-section datasets, such as radiochemical tracers.

"AWE has the capability to perform its own theoretical neutron cross-section calculations, through the use of publicly available and in-house modelling codes."

BOX 2

Neutron transport equation

The time dependent Boltzmann transport equation in energy group form can be expressed as:

$$\frac{1}{v_g}\left(\frac{\partial \phi_g(\underline{r}, \underline{\Omega}, t)}{\partial t}\right) + \underline{\Omega} \cdot \underline{\nabla} \phi_g(\underline{r}, \underline{\Omega}, t) + \sigma_g(\underline{r}) \phi_g(\underline{r}, \underline{\Omega}, t) = \sum_{g'=1}^{g'=G} \int \beta_{g'g}(\underline{r}, \underline{\Omega}' \rightarrow \underline{\Omega})\, \phi_{g'}(\underline{r}, \underline{\Omega}, t) d\underline{\Omega}' + S_g(\underline{r})$$

where the summation in the first term on the right hand side extends over G groups.

$\phi_g(\underline{r}, \underline{\Omega}, t)$ is the angular flux in neutron energy group g, at a time t, in unit solid angle about a direction $\underline{\Omega}$, at a point with position vector $\underline{r}$.

$\sigma_g(\underline{r})$ is the macroscopic total cross-section.

$\beta_{g'g}(\underline{r}, \underline{\Omega}' \rightarrow \underline{\Omega})$ is the transfer matrix (scatter + fission) which represents the scatter of neutrons in energy group g′, position $\underline{r}$ and direction $\underline{\Omega}'$ to energy group g, position $\underline{r}$ and direction $\underline{\Omega}$.

v_g is the velocity and $S_g(\underline{r})$ is a source term.

The main task of the Nuclear Data team is to provide the best available values for the quantities $\sigma_g(\underline{r})$ and $\beta_{g'g}(\underline{r}, \underline{\Omega}' \rightarrow \underline{\Omega})$. An example of the total cross-section has been shown in Box 1; an example of a transfer matrix is shown in Figure 3.

FIGURE 3

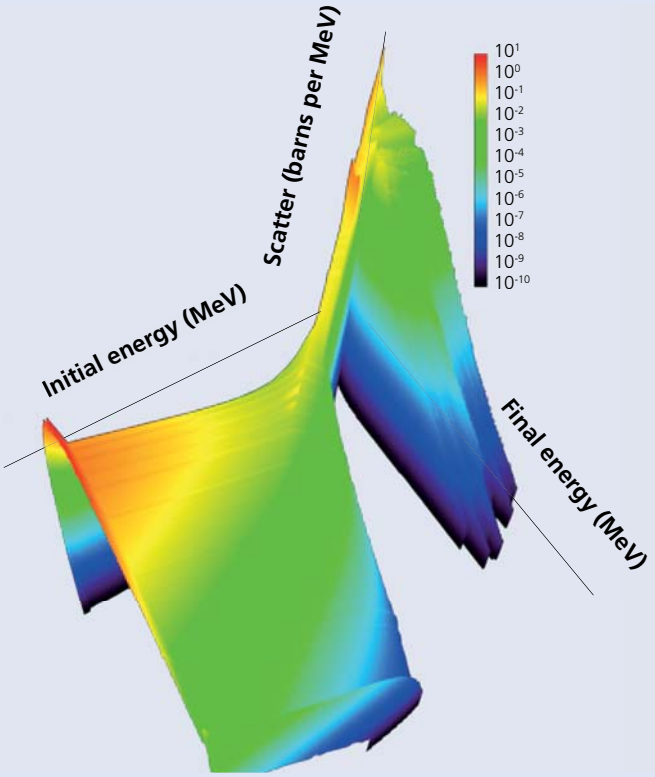

Example of a transfer matrix generated by the 3D graphics code NDview, showing the β scatter matrix for lithium-6 (^{6}Li) at a high temperature. At high initial energies the secondary distributions for threshold reactions, (i.e. inelastic scatter, (n, 2n), etc.), are visible. As the incident neutron energy decreases, the secondary distribution broadens indicating the enhanced upward and downward scatter due to thermal motion of the ^{6}Li nuclei. Energy scale in MeV decreases away from the origin.

BOX 3

Nuclear data codes

Specialised software has been developed over a number of years by AWE to process, manipulate and graphically display nuclear data. These codes have been developed, maintained and quality tested with the help of professional software consultants.

The main AWE codes are:

NDval: for validating the nuclear data produced in GENDF format by NJOY. A set of tests is applied to identify unphysical features or inconsistencies in the data.

NDconv: for conversion of data between different formats; in particular the conversion from NJOY generated GENDF format to AWE format.

NDxadj: for computing adjustments to data where necessary. The code iteratively compares calculated and experimental values of integral quantities such as critical assembly $k_{effective(s)}$ and produces a set of adjustments to provide the best fit.

NDLI: for applying adjustments if required, condensing to coarser group structures and combining libraries to create production libraries for use with AWE's modelling codes.

NDview: for graphical display of the data in 2D or 3D form. The code can read multiple formats and can perform a variety of operations on the data.

Benchmarking

Benchmarking is the definitive validation process for nuclear data and involves a comparison of results obtained through simulation with those obtained through experiment. This process is often employed during the release phase of a new nuclear data library as a method of verification and validation, and provides the end user with confidence that the data is consistent with physical quantities. Sensitivity studies may also be performed to provide a comparison between evaluated nuclear data libraries.

1D, 2D or 3D simulations are performed using a suitable neutronic modelling code and the results compared with a suite of experimental measurements. System eigenvalues such as $k_{effective}$ (a measure of system criticality) are often estimated as part of the validation process in addition to reactions rates, emission spectra and particle time of flight.

During benchmarking, it is important that the suite provides sufficient coverage of fissile materials, reflecting and moderating materials, neutron energies and material phases. This requirement is fulfilled by selecting a range of experimental systems including, bare/reflected fissile critical assemblies and high energy pulsed neutron systems.

ICSBEP provides an annual handbook containing benchmark specifications for experiments performed at various nuclear criticality facilities around the world [2]. The 'Jezebel' critical assembly was a near spherical, unreflected (i.e. bare), *δ-phase* ^{239}Pu experiment, operated throughout the 1950s at the Los Alamos National Laboratory (LANL). Designed to have minimal neutron reflection and highly reproducible results, many measurements were recorded including analytical eigenvalues ($k_{effective}$), neutron leakage spectra, and fission/activation reaction rates. Jezebel is considered to be one of the many experiments acceptable for use as a benchmark and features as one of the ICSBEP systems.

Neutronic modelling codes such as the LANL Monte Carlo Neutral Particle code – MCNP5 [3] – are often used to estimate integral quantities for critical or pulsed neutronic systems. A 3D model of Jezebel has been created at LANL using the MCNP5 code. Comparison of results obtained via simulation and experiment using three of the major nuclear

FIGURE 4

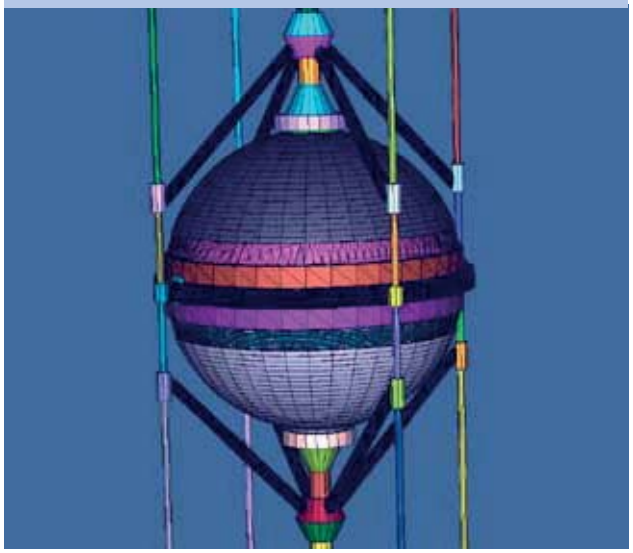

Plutonium-239 'Jezebel' Critical Assembly – complete.

FIGURE 5

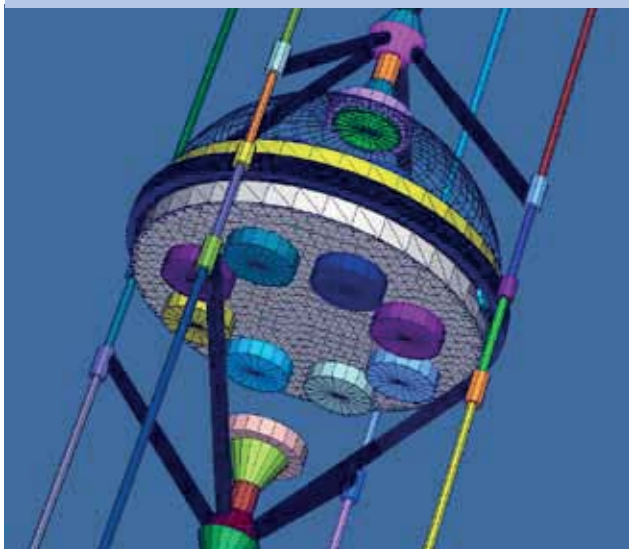

Plutonium-239 'Jezebel' Critical Assembly – hemisphere.

data libraries are given in Tables 1 and 2. The complex geometry associated with the Jezebel critical assembly is illustrated in the 3D visualisations provided in Figures 4 and 5.

The LINDA library and data assessment

In the past, comprehensive libraries derived from the JEFF, ENDF and JENDL evaluations have been made available for use with AWE's modelling codes. The data in these libraries differ and can produce significantly different results when applied to the same problem. While it is useful to have these 'independent' libraries, for comparison with US and European collaborators for example, a proposal was made in 2008 to select the most suitable data for individual nuclides chosen from the major evaluations, based on the findings of physics based assessments.

The Library of Individual Nuclide Data Assessments (LINDA) is AWE's answer to this requirement and are the data recommended for use in design calculations.

Nuclear reaction theory

Nuclear physics is one area of science in which theory still trails experiment. However, theoretical calculations of nuclear data quantities are still necessary in regimes not accessible to experiment, for example nucleons incident on a nucleus in a short term excited (i.e. metastable) state. AWE has the capability to perform its own theoretical neutron cross-section calculations, through the use of publicly available [4-6] and in-house modelling codes.

TABLE 1

Experiment	1.0000 ± 0.0020	
	$k_{effective}$	± 1σ
ENDF/B-VII	0.9986	0.0001
JEFF 3.1	0.9986	0.0001
JENDL 3.2	0.9964	0.0001

Plutonium-239 'Jezebel' $k_{effective}$ values.

TABLE 2

	σ_f (^{238}U)/ σ_f (^{235}U) Calc/Exp	σ_f (^{233}U)/ σ_f (^{235}U) Calc/Exp	σ_f (^{237}Np)/ σ_f (^{235}U) Calc/Exp	σ_f (^{239}Pu)/ σ_f (^{235}U) Calc/Exp
ENDF/B-VII	0.9673	0.9862	0.9830	0.9738
JEFF 3.1	0.9915	0.9980	1.0043	0.9832
JENDL 3.2	0.9833	1.0042	0.9751	0.9716

Central fission rates table.

Unfortunately, there is no 'one size fits all' nuclear theory and different theoretical models are required to cover different mass and energy regimes. Although many of the codes available are able to automatically select an appropriate model to use, an experienced operator is nevertheless essential in ensuring not only that the correct model is chosen, but also that the right choices of input and library parameters are made.

One nuclear model which is applicable to a large proportion of calculations is the Optical Model [7]. In this approach, the complicated potential energy field created by the nucleons within a target nucleus is approximated as a single mean field potential. A neutron incident on this nucleus will then only interact with a single potential, thereby simplifying the calculation substantially.

If this mean field potential contains both real and imaginary terms, the incident neutrons may undergo reactions into either an elastic or a non-elastic channel (covering all reactions other than elastic scatter). Other nuclear models may then be used to calculate the proportion of neutrons in the non-elastic channel which undergo each individual reaction type, for example (n, 2n), (n, inelastic).

For nuclear reactions involving low energy neutrons and/or low mass nuclei, the *R*-matrix [8] approach is favoured due to the presence of resolved resonances in these regimes. These resonances are difficult to predict using other theories, and if measured data are available their parameters may be used to better tune the theoretical *R*-matrix model.

The main use for AWE's theoretical capability is to assist in the validation of imported cross-section data and make informed choices about which datasets to select for LINDA, but it can also be used to generate data for nuclei where none currently exist.

Nuclear data uncertainties and their propagation in calculations

Neutron cross-sections, like any other physical quantity have an uncertainty associated with their true value. For experimentally derived data this uncertainty is due to measurement error while, for data calculated from theory, it arises from uncertainties in the parameters used in the modelling code.

As the nuclear data available within AWE's libraries are generally in group format, uncertainties are specified for the average cross-section of each energy group. This makes it especially convenient when taking into account 'covariance' (i.e. the correlation between the uncertainties in two different groups).

Covariance arises due to the fact that, in general, experiments to determine a cross-section at one energy are not independent of measurements made at a different energy. For example, a particular detector may produce a systematic error that extends over an energy range bridging several energy groups, leading to correlated uncertainties in the measured cross-sections in adjacent groups.

The covariance of two quantities, x_1 and x_2, is analogous to the variance of a single quantity, and may be written mathematically as:

$$\mathrm{cov}(x_1, x_2) = \sum_{i=1}^{n} \frac{(x_{1_i} - \overline{x_1})(x_{2_i} - \overline{x_2})}{n}$$

where, n is the number of measurements made of x_1 and x_2. The covariances in all of the energy groups for a cross-section may be stored conveniently in a covariance matrix, V_x:

$$V_x = \begin{pmatrix} \mathrm{var}(x_1) & \mathrm{cov}(x_1,x_2) & \ldots & \mathrm{cov}(x_1,x_n) \\ \mathrm{cov}(x_2,x_1) & \mathrm{var}(x_2) & \ldots & \ldots \\ \ldots & \ldots & \ldots & \ldots \\ \ldots & \ldots & \ldots & \mathrm{var}(x_n) \end{pmatrix}$$

where the diagonal terms are the variances and the off diagonal terms are the covariances between the measured quantities. It is often easier to visualise these matrices in 3D plots as shown in Figure 6.

The uncertainty in the nuclear data used in a calculation will lead to an uncertainty in the value of any quantity calculated using it. Covariance data can be used to calculate this uncertainty via the 'Sandwich Equation':

$$\sigma_y = \sqrt{\underline{D}^T \underline{V}_x \underline{D}}$$

where D and D^T are a vector of 'sensitivity coefficients' and its transpose respectively, and σ_y is the uncertainty (or standard

FIGURE 6

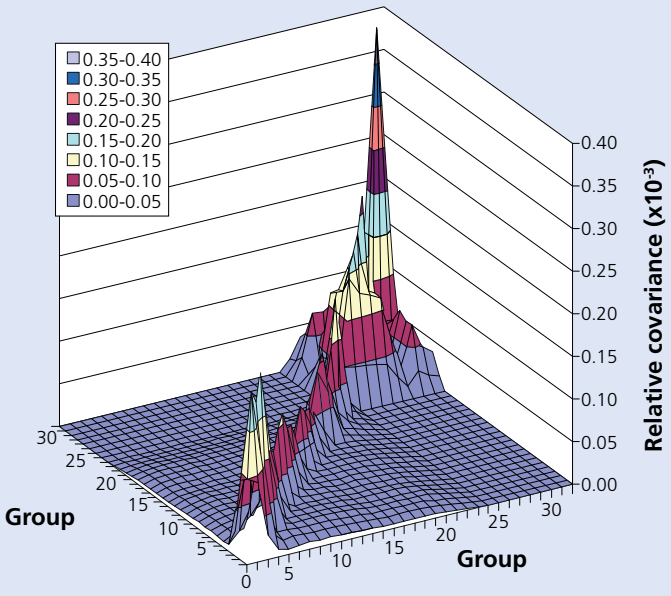

Plutonium-239 (n,f) relative covariance data from the ENDF/B-VII evaluation.

deviation) of some integral quantity which is the desired output of the calculation. These sensitivity coefficients are simply the rate of change of the integral parameter of interest with respect to cross-section for a particular energy group.

Covariance data from the ENDF/B-VII library have been used to successfully calculate the uncertainty of $k_{effective}$ for AWE's suite of critical assembly benchmarks [9]. The results of a subset of uranium benchmarks are given in Table 3 and show that in each case the uncertainty from propagated data errors exceeds the uncertainty from experiment.

Future work

LINDA is an evolving project and when significant new evaluations become available, the data will be assessed and, if deemed suitable, will be included in future library releases. NJOY processing skills are being developed to enable an in-house capability for future data acquisition.

Our data adjustment capability is being extended to include the use of data available from a wider range of experimental systems. To date only spherical (i.e. 1D) systems taken from the ICSBEP compilation have been used; a capability to include 2D systems has recently been implemented in NDxadj.

In the 1970s the Lawrence Livermore National Laboratory in the US undertook a programme of experiments measuring the neutron spectra produced when a wide variety of materials was bombarded with 14 MeV neutrons. These data give important information on neutron cross-sections at high energy; methods will be developed to exploit this experimental data, both for benchmarking and adjustment purposes.

Data uncertainty studies will be extended to cover more general non-linear cases where the use of the 'Sandwich Equation' may no longer be valid.

Although this article relates mainly to nuclear data activities in connection with neutron transport through materials, neutron interaction cross-sections are also used to modify the system nuclide inventory through transmutation reactions. An ongoing important and challenging task for AWE is to provide reliable cross-section sets, particularly for radiochemistry interpretation, which plays a pivotal role in its modelling capability.

TABLE 3

Sample	Reflector material	Thickness (cm)	Calculated uncertainty (%)	Experimental uncertainty (%)
1	Uranium	20.32	0.3993	0.3000
2	Polyethylene	1.45	0.3599	0.2800
3	Steel	9.70	0.3031	0.2400
4	Beryllium	4.70	0.3216	0.3000

Comparison of theoretical and experimental $k_{effective}$ percentage uncertainties for some uranium benchmarks.

References

[1] R.E. MacFarlane, D.W. Muir, The NJOY nuclear data processing system, LA- 12740-M (1994).

[2] J.B. Briggs *et al.*, International handbook of evaluated criticality safety benchmark experiments, NEA/NSC/DOC(95)04/I, Nuclear Energy Agency, France (2004).

[3] X-5 Monte Carlo Team, MCNP - A general Monte Carlo N-Particle Transport Code, Version 5, Los Alamos National Laboratory, LA-UR-03-1987 (2003).

[4] P.G. Young, E.D. Arthur, Proceedings of Computation and Analysis of Nuclear Data Relevant to Nuclear Energy and Safety, Trieste, Italy (1992).

[5] M. Herman, Proceedings of Workshop on Nuclear Reaction Data and Nuclear Reactors: Physics, Design and Safety, Trieste, Italy (2000).

[6] A.J. Koning, S. Hilaire, M.C. Duijvestijn, TALYS-1.0, Proceedings of the International Conference on Nuclear Data for Science and Technology, Nice, France (2007).

[7] A.J. Koning, J.P. Delaroche, Local and global nucleon optical models for 1 keV to 200 keV, Nucl. Phys. A 713, 231 (2003).

[8] A.M. Lane, R.G. Thomas, R-Matrix theory of nuclear reactions, Rev. Mod. Phys. 30, 257 (1958).

[9] J. Benstead, Nuclear data uncertainty propagation through a critical assembly benchmark suite, Proceedings of the International Conference on Mathematics and Computational Methods Applied to Nuclear Science and Engineering, Brazil (2011).

AUTHOR PROFILE

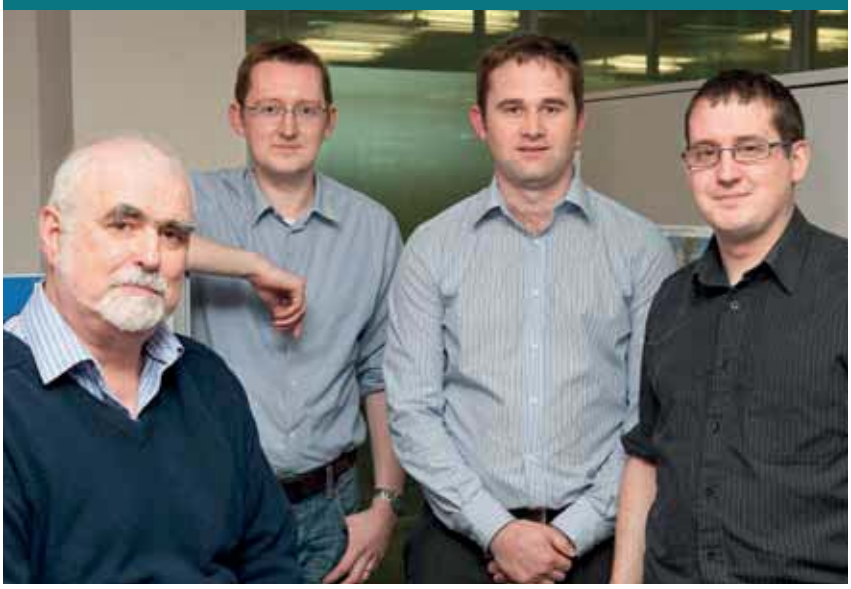

Left to right, Bruce Thom (Team Leader), James Benstead, Mark Jackson and Mark Cornock.

Bruce Thom

Bruce graduated from Edinburgh University with an honours degree in Physics in 1972 after which he moved to Queen Mary College in London to study for a PhD. He joined AWE in 1993 since when he has been principally responsible for the provision of nuclear data for AWE's modelling codes.

James Benstead

James graduated from the University of Lancaster with an MPhys (1st Class Honours). James joined AWE in 2006 and is currently undertaking a sponsored collaborative PhD at the University of Surrey studying the theoretical calculation of neutron interaction cross-sections.

Mark Jackson

Mark graduated from University College London with a BSc (1st Class Honours) in Physics. In 2007 he joined AWE and is currently working on the testing and benchmarking of nuclear data.

Mark Cornock

Mark joined AWE in 2006 after graduating with an MPhys in Physics with Planetary and Space Physics from the University of Wales. Since joining AWE Mark has principally been involved in the production and validation of nuclear data libraries.

Research into
Information Barrier Systems

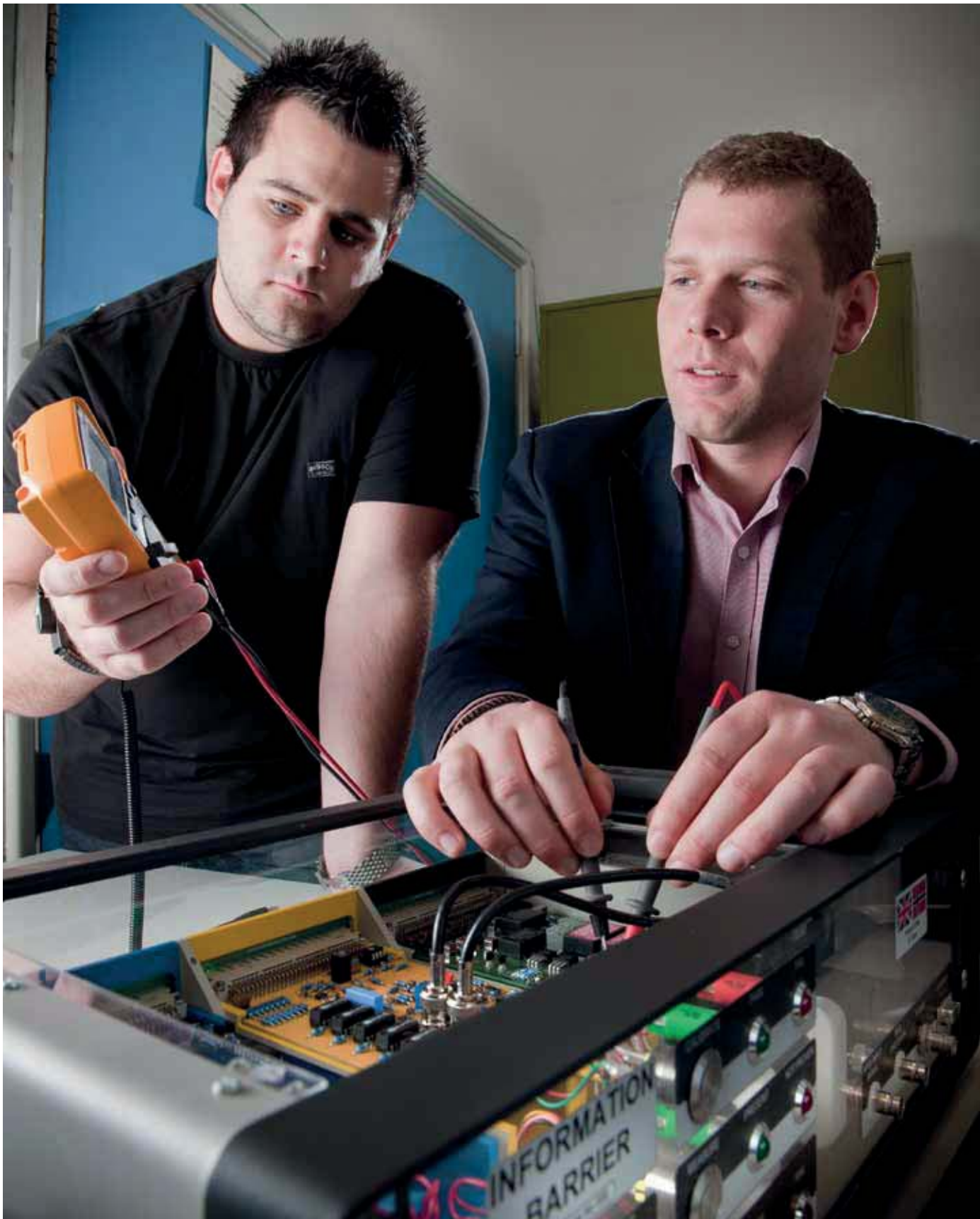

Any future nuclear disarmament process would need to be underpinned by a verification regime that can demonstrate with confidence that disarmament has taken place. With this principle in mind, the UK and Norway have been working together since 2007 in a unique and ground breaking technical collaboration to address some of the challenges that verifying the dismantlement of nuclear warheads could pose. This paper focuses an ongoing UK-Norway Initiative (UKNI) technical programme of work on the design and use of information barrier systems within a nuclear verification regime.

In a future verification regime for nuclear warhead dismantlement, inspecting parties are likely to request measurements on warhead and warhead components to ensure that the items presented are consistent with the declarations made by the host party.

Such measurements are likely to be based on radiation signatures, and would be used to confirm physical attributes of the fissile material present within the system.

Almost any measurement of this type would be likely to contain sensitive or proliferative information. It is therefore essential for such measurements to be performed behind an information barrier (IB) which, while protecting the sensitive information, will reveal whether the item(s) pass or fail to an agreed attribute threshold.

It is crucial that the IB design process builds in mechanisms whereby both parties can have high confidence in the validity of any result obtained during inspection.

This article highlights the outputs from the ongoing technical collaboration between the United Kingdom and Norway on the development of IB systems that can take trusted measurements on warhead or warhead components without revealing sensitive or proliferative information based upon their gamma ray emissions.

The requirements for an IB in an inspection regime raise complex issues and present significant design challenges. Aside from the obvious requirement that all equipment potentially used in a nuclear weapons production facility must be certified as safe, a number of additional constraints arise; these can be summarised into two types: design driven challenges and challenges in use. Of particular concern is the danger of using non-conforming equipment within an explosives area.

A key design challenge is that equipment used during measurements on a warhead or a warhead component is likely to be host supplied. This is primarily driven by the host's requirements for both safety and security, which in many cases will also be a legal requirement.

It is of course essential that any sensitive, potentially proliferative, information gathered is not released to inspectors; both the hosting and inspecting parties are responsible for ensuring compliance with these obligations.

It follows that the host may only permit the removal of inspection equipment by the inspectors when it can be proven that no sensitive information remained within the equipment.

An IB system requires a much greater degree of host and inspector trust than for systems which produce more detailed outputs (such as images, spectra or other detailed data).

"It is crucial that the IB design process builds in mechanisms whereby both parties can have high confidence in the validity of any result obtained during inspection."

The UKNI therefore produced a set of desirable qualities which would enable trust to be incorporated and these qualities applied during the development of the IB system.

Design driven challenges

A good IB design is trustable by both parties. The following points explore that definition and how the design concept can be developed to incorporate features that will assist with this.

- **Joint design**
  All aspects of the design and construction should be agreed by both parties. This enables both parties to have full design knowledge and therefore confidence in the accuracy of the system. It also allows ease of checking, both for the host party to certify for use and for the inspecting party prior to any measurements.

- **Modularity**
  Fast and simple interchange of modules allows random selection for checking the operation at any stage. Any modules that have not retained information can be returned to the inspectors after use, but only on the proviso that the host is confident that this is the case. Being able to check the equipment after use would be a substantial confidence builder for the inspecting party.

- **Simplicity**
  A simple design decreases the complexity of hardware and software verification. It also allows for all superfluous functionality to be removed from the equipment.

- **Inexpensive and commercially available components**
  Inexpensive components are essential if the equipment can only be used once or a limited number of times. The modular nature should reduce cost significantly by allowing much of the system to be reused after checking by both parties. Use of commercially available components also enables any party to buy and construct the system to the agreed specifications for their own further tests.

Challenges in use

The users of the IB must have confidence in its design. Therefore, design features of the mode of operation, many of which are obvious but frequently overlooked, should allow for reliable and repeatable operation.

- **Simple to operate**
  Clarity at all stages of a measurement is critical because any confusion over results or procedure could significantly affect the verification process.

- **Robust**
  The system needs to be reliable, operable in a variety of environments, and be able to withstand transportation.

- **Portable and self powered**
  The system needs to be easily portable, fast to assemble, and preferably not rely on host supplied power or other utilities to function.

- **Random selection**
  Random selection would allow the inspecting party to select from multiple copies of the equipment, or modules of the equipment, provided by the host. The inspecting party could choose which copy of the equipment would be used for measurements, and further copies for thorough checking potentially at their institute.

"Confirmation of the type of nuclear material present is the first step in building confidence that containerised objects presented for dismantlement could be warheads or warhead components"

The identification of plutonium

The first prototype system developed jointly by the UKNI in 2009 was designed to detect the presence of a given radioisotope.

Confirmation of the type of nuclear material present is the first step in building confidence that containerised objects presented for dismantlement could be warheads or warhead components, as declared by the host party.

Many gamma emitting radioisotope emits photons at well defined energies which can be used to uniquely identify the isotope present. Both parties agree the selection of energy peaks, which if present in a spectrum, would be used to confirm the presence of that particular isotope.

To verify the principle, an IB system was designed to detect the isotope cobalt-60 (^{60}Co); this selection allowed all the technical aspects to be discussed and developed, without any risk of discussing potentially sensitive or proliferative issues. The simplicity of this first test also provided a platform for more detailed discussions on authentication of the equipment, without needing to consider overly complex detection techniques.

It was agreed that the presence of ^{60}Co could be determined by the presence within the spectrum of peaks located at 1173 keV and 1332 keV, at a statistically reliable level above background.

When these peaks were detected the system output a green light indicting 'material present'; a red light would declare a 'not proven' result. This reflected the possibility that ^{60}Co could still be present, but at a concentration lower than the detection limit of the equipment.

The second prototype system incrementally built on the ^{60}Co algorithm to include the comparison against a pre-agreed ratio of two statistically valid peaks of two different isotopes. This version of the system increased the spectral resolution of the IB from 1024 to 4096 channels (from 1.6 keV per channel to 0.4 keV per channel). For this iteration of the IB system, sodium-22 (^{22}Na) 1275 keV and ^{60}Co 1332 keV peaks were used as surrogate plutonium isotopes. The system implemented a two peak calibration using europium (^{152} Eu) to maintain accuracy across the whole energy region of interest.

The third prototype system modified the surrogate algorithm to detect the presence of plutonium. It was proposed that the detection algorithms should have two main objectives when analysing a plutonium sample to:

- determine the presence of plutonium-239 (^{239}Pu),
- determine the isotopic ratio of ^{239}Pu to plutonium-240 (^{240}Pu).

In confirming the presence of ^{239}Pu and the isotopic composition of the sample, the IB was required to locate and analyse a selection of gamma ray peaks.

The device needed to be uncomplicated utilising only simple hardware and rudimentary software, which precluded the use of some of the more complex computational codes that were available.

Figure 1 shows a plutonium spectrum of one of the PIDIE standards (plutonium isotopic determination inter-comparison exercise). The plutonium spectrum contains several gamma ray peaks

FIGURE 1

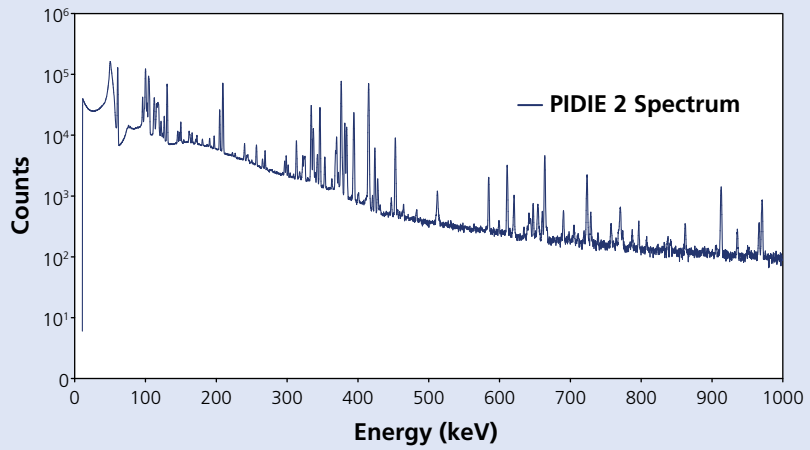

Plutonium spectrum showing an isotopic composition of PIDIE sample 2.

displaying spectral overlap; this is why a complex analysis code is often used to determine plutonium attributes.

To determine the presence of plutonium, and in particular ^{239}Pu, the IB system should search for a selection of the most intense gamma rays. Also perform a number of tests to study the shape, position and relative intensities of these peaks.

Not every gamma ray is unique and so it is possible that each of the peaks selected for use in identifying the presence of ^{239}Pu, could be from other radionuclides.

When considering the isotopic composition of plutonium, the most useful ratio exists between ^{239}Pu and ^{240}Pu. There are only four ^{240}Pu peak energy regions that can be considered: 45 keV, 104 keV, 160 keV and 642 keV. Peaks below 200 keV are often lost due to the absorption properties of any intervening materials which leaves only the peak at 642 keV. However, this region of the spectrum is complicated by several other gamma ray peaks due to ^{239}Pu and ^{241}Am, as shown in Figure 2.

In order to determine the isotopic ratio of ^{239}Pu to ^{240}Pu, the concentration of the materials present needed to be determined. Although this is relatively straight forward for ^{239}Pu due to the well defined peak at 645.89 keV which suffers no spectral overlap, it was more complicated for ^{240}Pu as the only peak in this region (642.35 keV) overlaps with ^{239}Pu at 639.97 keV and ^{241}Am at 641.47 keV. The ^{239}Pu contribution to the 640 keV region was calculated from the 645.89 keV peak and the associated branching ratios.

FIGURE 2

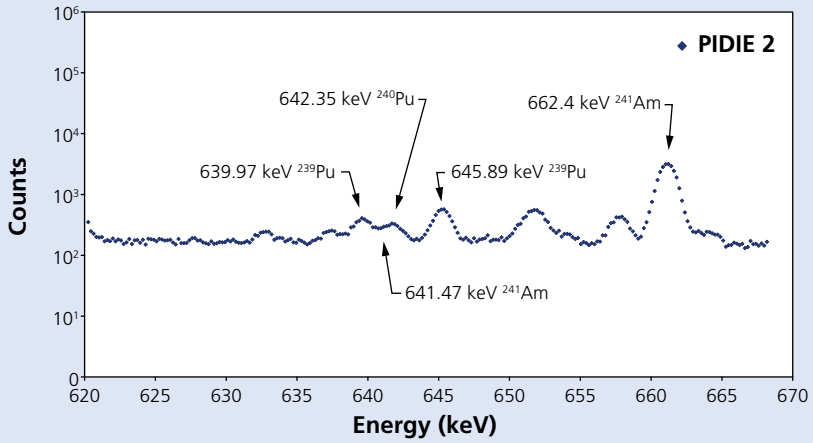

Gamma ray spectrum showing signals near 642 keV of PIDIE sample 2.

Similarly, the 662.4 keV ^{241}Am peak was used to calculate the ^{241}Am contribution, and therefore any other unaccounted peaks in the 640 keV region were attributed to ^{240}Pu allowing all isotopes of interest to be measured.

Information barrier implementation

The IB system consists of a standard high purity germanium (HPGe) detector interfaced with a custom designed and built IB electronics unit. The decay of radioactive material generates gamma photons which produce electrical pulses when they interact with the germanium crystal in the detector. These electrical pulses are then analysed by the IB electronics unit.

The IB electronics unit was developed by the joint UK-Norway IB team to enable the capture of the plutonium spectrum. A modular electronics design was developed consisting of analogue, digital and high and low voltage power supply subsystems.

The analogue subsystem interfaced to the HPGe detector and performed pulse capture, pulse shaping and peak detection operations. An analogue to digital converter (ADC) produced the digital signal for processing by the digital subsystem.

The digital subsystem captured the data from the output of the ADC and analysed the spectrum to determine the isotopic composition of the material in front of the detector. At the core of the digital subsystem was a simple microcontroller.

The AVR microcontroller was selected for the IB development as

it is one of the simplest commercially available controllers. Two versions of the software which the AVR executes have been developed for the IB. The UK developed version used the SPARK language whereas the Norwegian developed version used the AVR assembly language.

Associated with high consequence system development, AWE has long invested in a capability to develop high integrity software for simple control systems.

A key technology in AWE's high integrity development capability is the SPARK language and toolset. The SPARK language is a subset of Ada which is a language commonly used in defence and avionics systems where consequences of failure are high. SPARK also permits the use of annotations (essentially formalised comments) within the code, which enable the application of formal proof tools to verify that the code is correct.

The origins of the SPARK language are in systems developed on relatively primitive hardware platforms and as such was suited to the 8-bit AVR microcontroller in the IB system.

Typically, each SPARK module consists of two objects: a specification and a body. At its most basic level, a specification contains information about the functions and procedures that are defined in the corresponding body, such as function and procedure names, input/output parameters and their types.

A specification also provides the opportunity to declare more intent-like information about the functions and procedures. A precondition allows the programmer to further constrain any input parameters and, in the case of a function, a return assertion gives more information about the value returned by the function (with respect to its input parameters).

As well as ordinary program constructs, SPARK also allows the insertion of annotations in the code. Such annotations state what should be true of the local variables at the location of the annotation. Such annotations are used to prove properties about the implementation and its associated specification.

The next stage in the development process is to use the SPARK tools to check that the definitions above are well formed. The SPARK examiner will make some rudimentary checks to ensure that the code is syntactically correct.

From a verification perspective, the SPARK examiner will generate verification conditions that are required to be proven to ensure that the package fulfils all return assertions and annotations.

A second tool called the SPARK simplifier is available to prove as many of the verification conditions automatically. After simplification, the user is only required to prove those verification conditions that could not be proved automatically.

To do this, a tool called the SPARK proof checker assists the manual proof of verification conditions. It provides an interactive environment in which the user can submit proof commands to manipulate and, ultimately, prove verification conditions. Verification conditions can only be proven if they are true.

MALPAS

The principal disadvantage of using a high level programming language such as SPARK to write software is the necessity of a compilation phase in which the high level code is converted into machine instructions that can be understood by the AVR controller. This runs the risk of introducing errors into the software during compilation. In order to compare the advantages and disadvantages of this approach with one that eliminates the need for compilation the software for the Norwegian version of the IB was written directly in AVR assembly language.

The resulting code was greater in size and less readable than the corresponding SPARK, but was as efficient and still amenable to formal analysis by using tools such as MALPAS. A sample of the IB code was analysed using MALPAS to demonstrate this.

MALPAS is directly related to the SPARK tools, since both originated from the same research work. MALPAS was developed by the Royal Signals and Radar Establishment (RSRE) Malvern

and was targeted at the analysis of existing software, whereas SPARK was intended to be used during the development of software from the earliest specification stages. The MALPAS static code analysis tool can be used to analyse safety critical assembly code for in-service systems. The analysers determine various properties of the code ranging from basic topology to detailed mathematical functionality. They operate on a modelling language called 'intermediate language' (IL) which resembles a simple high level programming language with additional mathematical constructs.

The first stage of analysis is to translate the source code into IL. This is also very much an analysis stage in itself. By converting the source code into the more abstract IL model requires a precise understanding of the source code language and can start to highlight questionable areas in the software.

The MALPAS code sample analysis of the Norwegian IB was conducted in four main stages:

- Stage 1 involved manually translating the AVR assembly language to an IL model, as there is no automatic translator for the AVR assembly language.
- Stage 2 involved analysing the structure of the code and performing a relatively shallow check that the code meets its specification. The code identifies the expected inputs, outputs and information flow.
- Stage 3 of this study involved using the semantic analyser to examine execution time.
- Stage 4 covered proof of correct stack handling and use of the semantic analyser as an animation/testing tool.

The information flow analyser checks that the code complies with that specified in the PROCSPEC. The control flow analyser examines the topology of the IL PROC and indicates whether the code is well structured.

The data use analyser checks that the registers are being used according to their classification in the PROCSPEC. The MALPAS semantic analyser gives more detail about how the values of outputs are calculated.

The final stage of analysis involves adding more information to the IL model by providing semantics for the AVR instructions. The model is refined so that for selected AVR instructions it is stated exactly how they operate. This involves writing some supporting IL functions.

Testing the IB

The phase 1 IB system, as shown in Figure 3, was interfaced with a commercial HPGe detector; the IB was an all encompassing unit which included analogue signal manipulation and digital processing of the shaped pulses, and internal low and high voltage power supplies.

Figure 4 shows voltage pulses generated by the HPGe detector with each having a voltage proportional to the energy of the gamma photon that produced them.

The magnitude of the first peak is immaterial; instead it is the heights of the individual steps which are of interest, as shown in Figure 5.

Phase 1 of the IB was, in effect, a customised multi channel analyser (MCA) which incorporated: amplification and shaping of the incoming pulses, peak detection of the shaped pulses, analogue to digital conversion, discrimination of low/high channels and recording of the resultant spectrum.

"Associated with high consequence system development, AWE has long invested in a capability to develop high integrity software for simple control systems."

FIGURE 3

Phase 1 information barrier system.

MCAs usually have additional performance enhancing features such as pile-up rejection and sliding scale linearization, but such features were intentionally omitted from the phase 1 design, as the performance test required only basic MCA functionality.

Additional features would increase circuit complexity, and therefore increase the authentication effort. For manipulation of more complex spectra, such as that emanating from plutonium, a more precise MCA was needed.

The IB was designed to detect a pair of statistically valid peaks with regions of interest (ROI) centred on the ^{60}Co energies (1173 keV, 1332 keV). As such, there were various ways in which the instrument could fail to present a positive result, and tests were derived inline with these possibilities:

- ^{60}Co could be present, but at a concentration lower than the detection limit of the instrument. This would fail to generate a 'statistically valid' criterion. 'Statistically valid' requires each peak to pass the Currie Critical Limit test at 95%.
- No source is present with the instrument correctly determining this. ^{60}Co could be present, but fall outside the required ROI due to drift following calibration.

Alternatively, the following scenario could give a positive result when ^{60}Co was in fact absent:

- ^{60}Co could be absent, but an isotope having peaks nearby to the chosen ROI could be present.

Introduction of role playing between host and inspector

The intended use of an IB system assumes access restrictions of the item to be interrogated. Phase 1 introduced the aspect of host/inspector roles by providing unknown sources to the inspecting party.

This was in line with the IB design, allowing no prior knowledge of the item under question to influence equipment initialisation. The easy of operation and clarity of the system's outputs were tested in the 2009 UK Norway managed exercise.

FIGURE 4

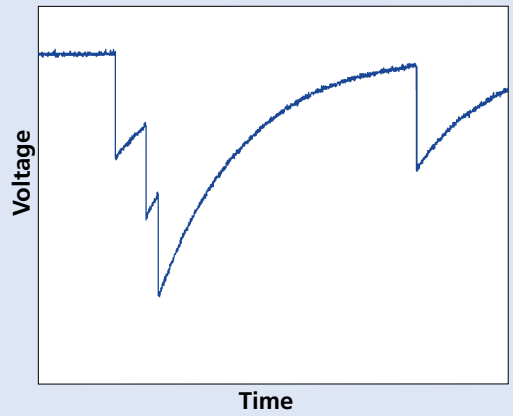

Voltage pulses generated by the HPGe detector.

FIGURE 5

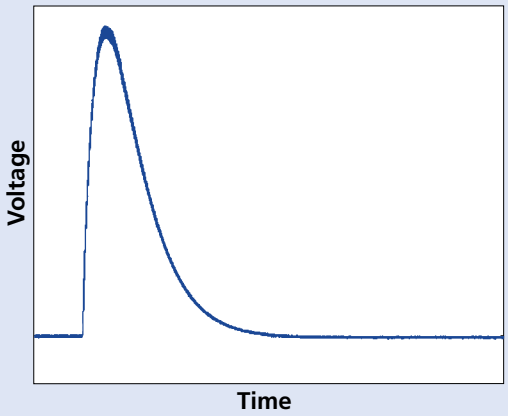

Peak shaping pulse.

Overall the phase 1 IB system met operational requirements confirming its suitability for identifying ^{60}Co, but was inappropriate for more complex tasks. This highlighted the compromise required between simple implementation, ease of authentication and increased performance.

Detector overload

Shutdown, due to detector overload, can occur in the presence of high activity sources. If the approximate activity is known, shielding, or increased distance may offer a partial or complete solution. It is very unlikely that the exact source activity of a treaty accountable item will be known by inspectors; in order to provide meaningful results, detector stand-off distances need to be adjusted depending on the situation.

An IB should preclude all detailed spectral information from being monitored during measurements. However, for developmental purposes, such information is essential.

Phase 1 of the IB was able to distinguish between gamma peaks of different energies, whilst phase 2 was designed to distinguish between different peak energies as well as measure peak areas accurately.

Figure 6 shows the phase 2 IB which was designed to test the iteration's ability to compare two peak net areas. Specifically, the phase 2 IB was required to light the 'present' LED if the net area of the 1275 keV ^{22}Na peak was less than the agreed isotopic ratio of the 1332 keV ^{60}Co peak, and the 'not proven' LED if greater or if the confidence in an individual measurement was lower than 95%.

Since sets of homogenous sources having different ^{22}Na/^{60}Co ratios are not readily available, a pair of uncalibrated sources, approximately 74 kBq, was deployed; the position of the ^{60}Co was fixed whereas the position of the ^{22}Na was variable. The purpose of this was to obtain a controllable ratio between the two peaks by changing the source separation. The ^{22}Na/^{60}Co ratio reported by the MCA via Ortec Maestro was used as the reference ratio.

A total of 145 tests were conducted, with the majority clustered around the decision region; accounting for some minor discrepancies both IBs performed exactly to specification. An accurate assessment of IB performance requires a great deal of reliable data to be acquired in a limited time frame. The tests therefore needed to be as simple as possible and implemented with a minimum of lost time between counting. Figure 7 shows the physical arrangement of sources.

During the phase 2 trials in Norway, a single HPGe detector supplied a distribution amplifier enabling two IB systems to process the same data, allowing more accurate comparisons to be made.

The IB tests were conducted in groups of five; the measured probability of lighting the 'present' LED could be calculated for each group of five tests. Since the tests were conducted in groups of five, the obvious candidate is the average of the measured ^{22}Na/^{60}Co ratios as measured by the reference MCA for those five tests as shown in Figure 8.

FIGURE 6

Phase 2 information barrier system.

The graph shows a solid 'present' light until the $^{22}Na/^{60}Co$ ratio exceeds the agreed isotopic ratio, whereupon the probability of the 'present' light lighting becomes zero, and the 'not-proven' light lights.

Although the IB measures and makes decisions on $^{22}Na/^{60}Co$ ratios to 100% confidence well away from the agreed isotopic ratio transition region, behaviour in the transition region is important as shown in Figure 9.

The transition region has a defined width and gradient. More significantly, all but one of the non-zero probability points occurs below the agreed isotopic ratio because the 'not proven' LED will most likely illuminate if the $^{22}Na/^{60}Co$ ratio exceeds the agreed ratio.

There were 145 tests divided into 29 groups of five. The specification required a 95% confidence of obtaining the correct result, which is equivalent to a 1 in 20 chance of an incorrect result. Thus, in 29 groups, one incorrect result was expected. The data demonstrated that 95% confidence in the declaration algorithm was achieved.

Conclusions and future work

There are various factors that have positively influenced the UK-Norway collaboration. Whilst the multinational project team is forging a working relationship it is vital to limit the scope of the deliverables and then iterate through the development life cycle to incrementally evolve the system into a fully operational solution.

Full participation by both parties is critical as both require a full working knowledge of the system to understand areas of potential exploitation by subversive actions, to reconcile any potential performance limits and to inform the authentication and certification processes.

The performance of the proposed plutonium algorithm has demonstrated through simulation that it will confidently return the correct results for a given range of isotopic ratios with a range of

FIGURE 7

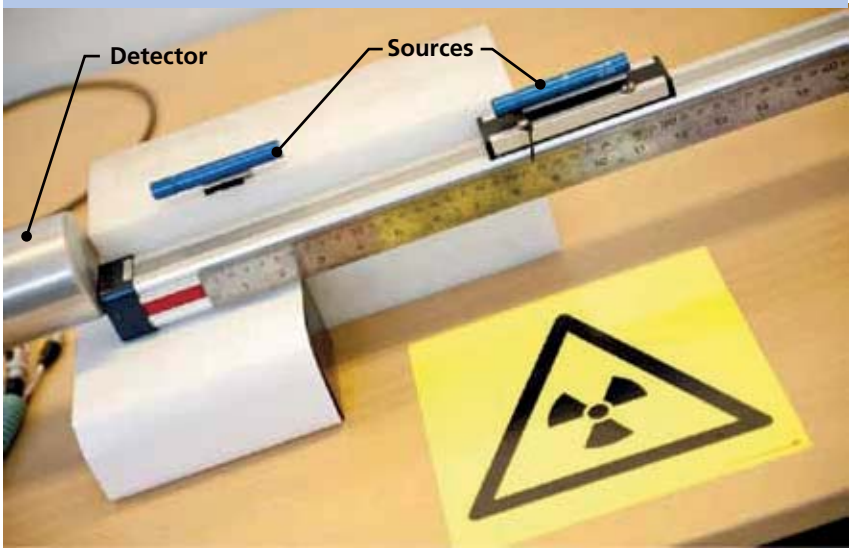

Physical arrangement of sources.

FIGURE 8

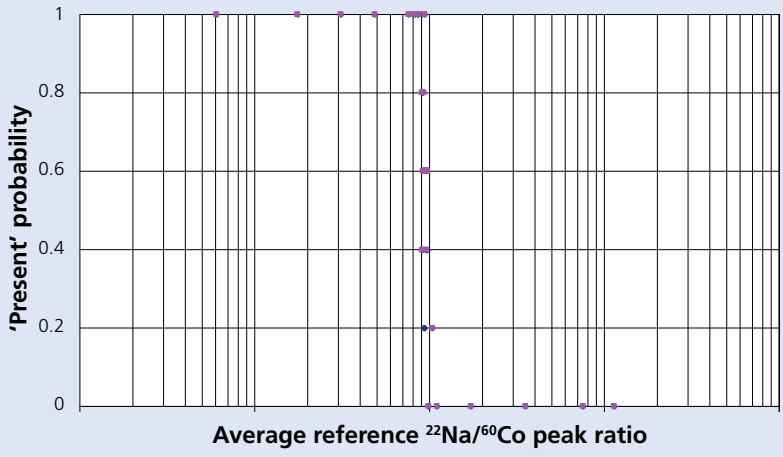

Information barrier 'present'/'not proven' transfer characteristic.

radiation background levels. The next task is to perform a measurement campaign to validate the algorithm performance.

Verification of particular isotopes being present and of material grade builds confidence, but is only a start. Further development of systems which are able to determine if there is an over declared threshold mass of fissile material, if an age threshold is exceeded, or which could confirm previous measurements, would build further confidence. These may need to study other signatures beyond those available in the gamma spectrum. The commercial detectors will also need examining for building confidence in their veracity. Those detectors with complex electronics or software will negate the effectiveness of the IB, as it will not be possible to ascertain if the detector itself has been altered.

The UK and Norway will continue to study procedures and protocols for use of the IB system in a disarmament context. The IB system itself cannot instil or maintain trust in its accuracy and truthfulness; only by robust and mutually agreed procedures can the system be trusted.

FIGURE 9

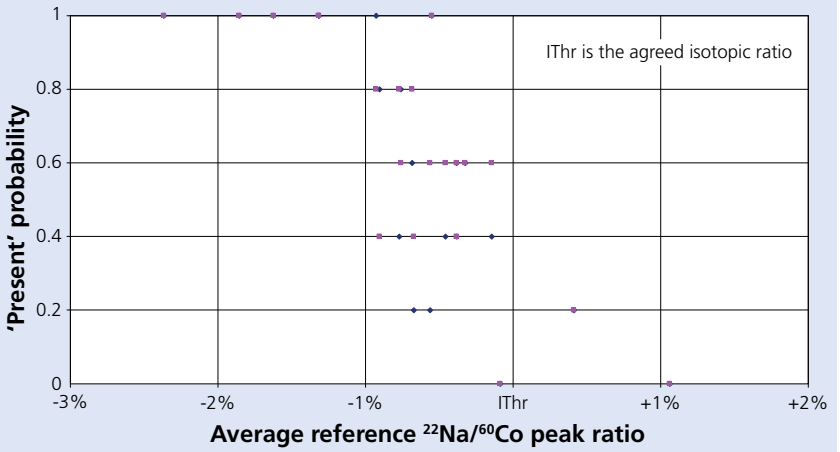

Detail of the transition region.

The UKNI

At the 2005 Review Conference of the Parties to the Non-Proliferation Treaty (NPT), the UK Government expressed an interest in exploring opportunities for interchange with other governments and state organisations in the field of nuclear arms control verification.

In late 2006, this led to representatives of the Norwegian Radiation Protection Authority (NRPA), the Ministry of Defence (MOD) and the Verification Research, Training and Information Centre (VERTIC) instigating a technical exchange between the UK and Norway in this field.

The Norwegian Defence Research Establishment, Norwegian Seismic Array and NRPA met with representatives from the MOD, AWE and VERTIC to discuss a potential cooperation on matters related to the technical verification of nuclear arms control.

The Norwegian researchers were particularly interested in investigating how a non nuclear weapons state (NNWS) could play a constructive role in increasing confidence in the nuclear disarmament process of a nuclear weapons state (NWS). It was agreed that an unclassified exchange within this field of research was feasible and that a programme of work should be developed. It should be noted that this is the first time a NWS and NNWS have attempted to collaborate in this field of research. Under this initiative, two areas of research have so far been undertaken: information barriers and managed access.

Managed access is the process by which 'uncleared' personnel are given access to sensitive facilities, or supervised areas, under the terms of an agreed procedure or protocol. A managed access familiarization visit exercise took place in Norway in December 2008, allowing an 'inspecting party' (the UK taking the role of a NNWS) to become familiar with the mock-up facilities controlled by the 'host party' (Norway taking the role of a NWS), and to prepare for a follow-on monitoring visit. The follow-on managed access monitoring visit

exercise was held at the mock-up nuclear weapon dismantlement facility in Norway in June 2009.

Two jointly designed IB prototypes were tested during the monitoring visit exercise; this was the first field test of the IB technology developed as part of the UKNI. The UKNI presented the outcome of the planning, conduct and evaluation of the 2008/2009 managed access exercises at the 2009 NPT preparatory committee meeting and the 2010 NPT review conference.

Following on from the 2009 exercise, the UKNI collaboration undertook a further 'focused' exercise which explored the impact of host security measures on the inspection regime, and demonstrated some aspects of the safety regulatory environment associated with a nuclear weapons complex. The exercise showed how the security/safety regime implemented by the host state could impact on the inspectors' ability to assess the potential threats to, and vulnerabilities of, a potential future monitoring regime.

A comparison between the adversarial environment of the 2010 exercise and the collaborative environment of the 2008/2009 exercises indicate that a collaborative environment, and a proactive host, could help to facilitate the inspection process and increase inspector confidence levels. In conclusion, the managed access project has provided opportunities for Norwegian and UK participants to explore issues relating to nuclear arms control verification without the risk of proliferation, and has promoted a common understanding within the UKNI of the issues faced by each party. This is essential for technology and procedural development in the future.

Acknowledgments

The work presented in this paper is a summary of the achievements of the UKNI on developing IB technologies.

AWE is very grateful to our friends and colleagues from all the organisations within the UKNI for allowing us to publish this work.

Recommended reading

The United Kingdom – Norway Initiative: research into the verification of nuclear warhead dismantlement, Working paper to the Non-Proliferation Treaty Review Conference, NPT/CONF2010/WP.41 (May 2010).

O. Reistad *et al.*, UK-Norway Initiative: research into managed access of inspectors during warhead dismantlement verification, INMM 51st Annual meeting, Baltimore, MD, USA (July 2010).

D.W. MacArthur, J.K. Wolford Jr., Information barriers and authentication, INMM 42nd Annual meeting, Indian Wells, CA, USA, (July 2001).

J. Barnes, High integrity software - The SPARK approach to safety and security, Pearson Education (2003).

Joint DOD/DOE information barrier working group, Functional requirements and design basis for information barriers, PNNL-13285, PNNL, Richland, WA, USA (May 1999).

D.G. Langner *et al.*, Attribute verification systems with information barriers for classified forms of plutonium in the trilateral initiative, Symposium on International Safeguards, Vienna, Austria (Oct- Nov 2001).

S. Backe *et al.*, The United Kingdom - Norway Initiative: further research into managed access of inspectors during warhead dismantlement verification, INMM 53rd Annual Meeting, Florida, USA (July 2012).

H. White *et al.*, Research into nuclear arms control verification at the UK Atomic Weapons Establishment, INMM 50th Annual Meeting, Tucson, AZ, (July 2009).

D.M. Chambers *et al.*, UK-Norway Initiative: research into information barriers to allow warhead attribute verification without release of sensitive or proliferative information, INMM 51st Annual meeting, Baltimore, MD, USA (July 2010).

AWE's Outreach, Major Events and Collaborative Activities

A few key events in which AWE participated during the later part of 2011 and the early part of 2012 are presented.

Conference on Nuclear Criticality Safety

AWE sponsored the 9th International Conference on Nuclear Criticality Safety held on 19-23 September 2011 in Edinburgh.

The conference was attended by 273 delegates from 21 countries. This was an opportunity for AWE to showcase its capabilities in criticality safety and four presentations were provided.

The conference was a resounding success and feedback has been extremely positive. Furthermore, AWE has been invited to participate in various aspects of the US Nuclear Criticality Safety programme.

Materials conference agrees international standards

Co-sponsored by AWE, the 18th Plenary Meeting of the International Standards Organisation Technical Committee 202 (ISO/TC202) was held at the National Physical Laboratory (NPL) on 18-20 October 2011. It was the first time that the meeting had been hosted by the UK for over 10 years.
The UK has been an active member of the committee since 1992. TC202 covers all aspects of microbeam analysis.

AWE Materials Scientist and ISO/TC202 working group convener, Mike Matthews, said: "This field of work is a key component in delivering AWE's technical programme. The plenary meetings are an important and integral part of the international standards creation process. Without the voluntary contributions made by our experts, the UK would have no say on the content of these standards."

A delegation of over 40 experts in microbeam analysis attended the conference, with representatives from China, France, Germany, Japan, South Korea, South Africa, UK and the US.

Minister welcomes collaboration on laser fusion energy

A memorandum of understanding (MoU), which will see AWE collaborating with UK and US physicists in the quest for viable laser fusion energy, has been welcomed by David Willetts MP, Minister for Universities and Science.

The MoU – signed between AWE, the Science and Technology Facilities Council (STFC) and Lawrence Livermore National Laboratory (LLNL) – will facilitate technical exchanges which could lead to the design, development and deployment of power plants based on laser fusion energy.

Collaboration will involve AWE's Orion laser facility, the STFC led High Power Laser Energy Research Facility (HiPER) and the National Ignition Facility (NIF), hosted by LLNL.

The ultimate aim is to demonstrate the technical and economic viability of laser fusion as a source of commercial energy production.

Over 180 experts and industry professionals, including members

ISO/TC202 Materials Conference

Laser Fusion Energy Conference

of AWE's physics community, gathered at The Royal Society, London, on 07 September 2011, for a conference under the banner 'Laser energy – an opportunity for UK industry.'

Speaking at the event, Mr Willetts said the Government understood the importance of a secure, reliable and affordable energy supply and laser energy had the potential to make a major contribution.

"Commercially, the UK could be a big player in the global laser market which is a very exciting prospect. We are at the heart of international collaboration in laser fusion energy."

"I hope this MoU between AWE, STFC and LLNL will be a precursor to closer collaboration between the UK and US."

"I am very pleased that beamtime from the new Orion laser at AWE will be available for academics – supporting this very important technology."

Hydrodynamic simulations conference

Following on from successful meetings in Paris, Oxford, Prague and Pavia, the International Conference on Numerical Methods for Multi-Material Fluid Flows (Multimat 2011) was held on 05-09 September 2011 in Arcachon, France.

Discussions were held on a number of topics including numerical methods for multi-material hydrodynamics. A number of AWE design physicists gave presentations on this important area of research.

AWE participates in high level physics conference

For the third year running, AWE co-sponsored the Institution of Physics' Condensed Matter Materials Physics conference (CMMP), held on 13-15 December 2011, at the Lancashire County Cricket Ground, Manchester.

AWE hosted the 'Matter under Extreme Conditions', chaired this year by Distinguished Scientist, Professor Neil Bourne.

Through an invitation facilitated by AWE, Professor Yogi Gupta of Washington State University gave the plenary talk. Professor Gupta is considered a world expert in the shock physics field.

The highlight of the session was a presentation by Professor Malcolm McMahon from Edinburgh University who spoke about some unusual behaviour in solids that had recently been discovered at high pressure. Professor McMahon has joined AWE as a William Penney Fellow.

Other AWE contributors included Caroline Shenton-Taylor discussed novel diagnostics to measure temperature in shock experiments and Seyi Latunde-Dada who described experimental and theoretical hypervelocity

impact. However, the condensed matter physics work at AWE is not limited to studying matter at extreme conditions, as shown by Tony Devey who gave a presentation in the 'Surface Science' session.

Once again, CMMP proved extremely successful and presented opportunities to engage with the academic community. This was demonstrated by the calibre of the invited speakers – supporting AWE's growing reputation in the field of condensed matter.

Celebrate at AWE 2011

The Celebrate at AWE Awards took place on 23 September 2011 at Newbury Racecourse – marking a celebration of the excellent work, commitment and dedication of our people – at the workplace and in the community. The awards were opened by AWE's Managing Director, Doctor Andrew Jupp, who took the opportunity to thank staff for their contributions in transforming AWE – helping to improve and develop the way that AWE works, creating more efficiencies and working smarter.

Doctor Jupp recognised the loyalty and commitment of employees across AWE and thanked staff for their contribution and achievements during the year.

The MOD's Strategic Weapons Project Team sponsored the Chief Scientific Adviser Ministry of Defence Award, which was presented by Director of Strategic Technologies, Peter Sankey OBE.

The Clive Marsh Award for innovative contribution demonstrating creativity at early career stage, was awarded to Doctor Peter Bolton.

The two JC (Charlie) Martin Awards recognise technical content, originality and presentation in an internal or externally published paper. The best external paper was awarded to Doctor David Green and Doctor David Bowers. The best internal paper went to Cassie Parrish.

The Chief Scientific Adviser Ministry of Defence Award, for pioneering breakthrough or discovery in the SET field was presented to Doctor Peter Harrison, Tom Boon and Dean Pask (main photograph page 48).

The John Challens Medal, which recognises sustained, high quality and valued contribution to the work of AWE in the SET field was awarded to Professor Peter Roberts.

Gold award team winners

Discovery

Find out more about AWE at our website:

www.awe.co.uk

Comments and suggestions regarding this journal, please email:

discovery@awe.co.uk

For further copies of this journal and details of other AWE publications, please write to:

Corporate Communications Office
Building F161.2
AWE Aldermaston
Reading
Berkshire
RG7 4PR

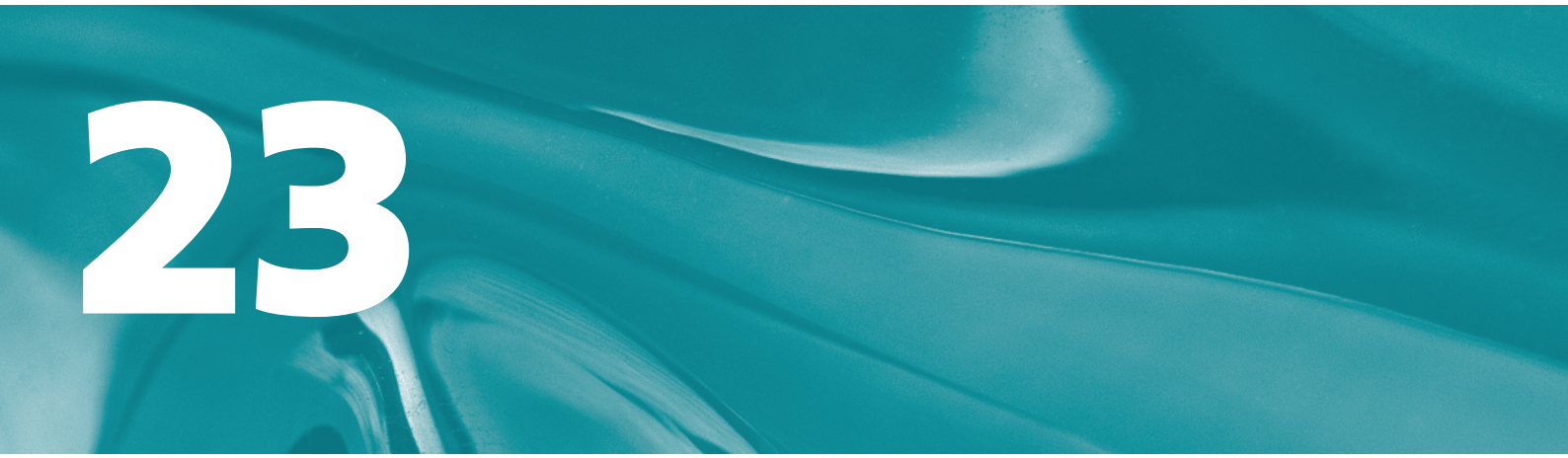

Printed on Greencoat silk

AWE is the trading name of AWE plc
Registered office: Aldermaston Reading Berkshire RG7 4PR
Registered number 3664571

The Science & Technology Journal of AWE • Issue 23 • July 2012